

**OPTIMUM RETROFITTING METHODS FOR  
LOW RISE MASONRY STRUCTURES IN SRI LANKA**

Gihan Bhashitha Ranasinghe

(198008E)

Degree of Master of Science

Department of Civil Engineering

University of Moratuwa

Sri Lanka

May 2020

**OPTIMUM RETROFITTING METHODS FOR  
LOW RISE MASONRY STRUCTURES IN SRI LANKA**

Ranasinghe Mudiyanseelage Gihan Bhashitha Ranasinghe

(198008E)

Thesis submitted in partial fulfilment of the requirements for the Degree of Master of  
Science in Civil Engineering

Department of Civil Engineering

University of Moratuwa


Sri Lanka

May 2020

## Declaration of the Candidate & Supervisors

I declare that this is my own work and this thesis/dissertation does not incorporate without acknowledgement any material previously submitted for a Degree or Diploma in any other University or institute of higher learning and to the best of my knowledge and belief it does not contain any material previously published or written by another person except where the acknowledgement is made in the text.

Also, I hereby grant to University of Moratuwa the non-exclusive right to reproduce and distribute my thesis/dissertation, in whole or in part in print, electronic or other medium. I retain the right to use this content in whole or part in future works (such as articles or books).

Signature: 

Date: 24.06.2020


The above candidate has carried out research for the Master's thesis under our supervision.

Name of the supervisor: Prof. Mrs. C. Jayasinghe

Signature of the supervisor: 


Date: 26.06.2020

Name of the supervisor: Prof. M.T.R. Jayasinghe

Signature of the supervisor: 

Date: 26.06.2020

Name of the supervisor: Prof. P. Walker

Signature of the supervisor: 

Date: 27 June 2020

## **ABSTRACT**

Floods can be considered as one of the natural hazards which cause destructive effects on the existence of mankind. Most of the mortalities have taken place due to damages in masonry walls of unreinforced masonry structures. These walls have failed due to its insufficient capacity to resist lateral forces exerted by floods. A field survey that was carried out in houses damaged due to flood revealed that, the outermost walls can play a major role in reducing flood induced damage, if they are strengthened to resist lateral forces applied by floods. Retrofitting of masonry walls has been recognized as a possible solution to strengthen the masonry structures against the aforementioned forces. Many researches have done in the past to strengthen the masonry walls by using different retrofitting types. Most of them are limited only to in plane behavior of walls with retrofitting.

The study has focused on the out of plane loading exerted by flooding. The failure mechanism due to floods was identified as the flexure parallel to bed joint of the masonry based on the field study conducted in the flood affected areas of Sri Lanka. The experimental program was mainly focused on flexure parallel to bed joint. Fired Clay Bricks (FCB) and Cement Blocks (CB) were used as the walling material for panels, whereas geogrid and wire mesh were used as the retrofitting materials for the research. The FCB panels retrofitted with geogrid and rendering under saturated conditions have shown an increase of 9.2 times the flexural strength of the reference wall panel without any retrofitting which is subjected to saturated condition and 6.78 times for the wire mesh. For CB, it was 5.8 times and 4.5 times respectively. The results have indicated that the masonry houses can be retrofitted and deployed to protect the people from floods.

Keywords— Brick, Cement block, Flexural strength, Flooding, Masonry, Retrofitting

## **ACKNOWLEDGEMENTS**

The funding provided by the Royal Society (Global Challenge Research Fund) for the project “Safer communities with hydro-meteorological disaster resilient houses”.

Under the Research Project, I had the opportunity of gaining a very valuable experience of how to apply the theoretical knowledge gathered throughout the four years as an undergraduate to produce important findings for the well-being and development of the community.

There are number of persons whom I must pay my sincere gratitude for their help towards the successful completion of this research project and report.

First and foremost, I would like to express my heartfelt gratitude to my research supervisors Prof (Mrs.) C. Jayasinghe Senior Professor in the Department of Civil Engineering, University of Moratuwa, Prof. M. T. R. Jayasinghe, Senior Professor in the Department of Civil Engineering, University of Moratuwa and Prof. P. Walker, Professor in the Department of Architecture and Civil Engineering, University of Bath who granted me the invaluable opportunity to carry out this research. This research project would have never been succeeded without your assistance and guidance in every step throughout the project.

I would like to deeply appreciate Dr. Shawn Platt, Research Associate, Department of Architecture and Civil Engineering, University of Bath who provided the support, guidance and advices in many occasions and providing worthy ideas and solutions for the problems which arose in the project.

I gratefully thank to Dr. Dan Maskell, Department of Architecture and Civil Engineering, University of Bath who encouraged us to complete this project successfully.

I am thankful to Dr. H.G.H. Damruwan and Dr. J.C.P.H. Gamage for evaluating and giving me valuable instructions regarding the research findings I have in this research study.

I would like to show my profound gratitude to Ms. K.P.I.E. Ariyaratne and Mr. H.A.D.G.S. Jayathilake who gave me a tremendous support to conduct the research throughout the year.

Finally, I pay my appreciation to Mr. N.L. Dissanayake, Mr. H.T.R.M. Thanthirige, Mr. M.L. Perera, Mr. P.P.R. Peris, Mr. L.H.K. Chandana and all other non-academic staff of Department of Civil Engineering, University of Moratuwa who helped me in experimental work.

Thank you,

R.M.G.B. Ranasinghe

198008E

Department of Civil Engineering

University of Moratuwa

20.06.2020.

# TABLE OF CONTENTS

Declaration of the candidate & supervisors .....	I
Abstract .....	II
Acknowledgements.....	III
1. Introduction.....	1
1.1 Research background .....	1
1.2 Masonry structures .....	2
1.3 Objective.....	4
1.4 Methodology.....	4
1.5 Arrangement of the thesis.....	5
2. Literature review.....	6
2.1 Introduction.....	6
2.2 Investigate the magnitude and the nature of the damage, types of structures affected, impact on human lives in post disaster stage .....	7
2.3 Unreinforced Masonry (URM) structures .....	8
2.3.1 Forces acting on urm walls.....	9
2.3.2 Out of plane behavior of masonry walls .....	10
2.3.3 Retrofitting of URM structures .....	16
2.4 Summary.....	21
3. Field study.....	22

3.1	Introduction.....	22
3.2	Field survey .....	22
3.3	Study area .....	22
3.4	Data collection and survey format .....	23
3.5	Analysis of results .....	25
3.5.1	Geographic data.....	25
3.5.2	Details of surveyed flood affected houses .....	28
3.5.3	Certificate of Compliance (CoC).....	32
3.5.4	Physical observations due to flood .....	33
3.5.5	Physical impacts .....	35
3.5.6	Socioeconomic impacts.....	38
3.6	Proposed solution for flood resilience.....	40
4.	Experimental study .....	41
4.1	Introduction.....	41
4.2	Materials used for the study.....	41
4.2.1	Masonry units .....	41
4.2.2	Mortar .....	50
4.2.3	Retrofitting materials.....	58
4.3	Construction of masonry wall panels.....	60
4.4	Testing of wall panels for flexure parallel to bed joint .....	63
4.5	Experimental results .....	64
4.6	Analysis of experimental results .....	66
4.6.1	Strength increase in flexural strength (parallel to bed joint) with different types of retrofitting.....	67



4.6.2	Impact of saturation of wall panels under flood situation.....	69
4.6.3	Failure types observed in wall panels during the experimental program ....	70
4.6.4	Cost study.....	73
5.	Practical application of the outcome from the experimental program.....	74
6.	Conclusion and future work .....	77
6.1	Conclusion .....	77
6.2	Future work.....	78

## LIST OF FIGURES

Figure 2. 1: Prevailing studies relevant to masonry structures	6
Figure 2. 2: Arrangement for the testing	11
Figure 2. 3: Structural functioning of reinforced masonry wall subjected to loading (out-of-plane)	12
Figure 2. 4: Failure of the reinforced wall due to shear	13
Figure 2. 5: Testing arrangement of the wall panels	14
Figure 2. 6: Annual time series for damaged or destroyed houses in Sri Lanka due to disasters (excluding Tsunami)	15
Figure 2. 7: Profile of houses destroyed and damaged due to disasters excluding tsunami: 1974 -2008	15
Figure 2. 8: Set up for static cyclic load test	18
Figure 2. 9: Test apparatus with CFRP applied to wall	21
Figure 3. 1: 2017 Flood level in Kalutara district, Source: BBC	22
Figure 3. 2: Survey Locations	23
Figure 3. 3: Different attributes of the survey	25
Figure 3. 4: Percentage of houses which are within the distance of 1 Km and more than 1 Km to the closest body of water	26
Figure 3. 5: Elevation from river water level (in ft)	27
Figure 3. 6: Types of access roads	27
Figure 3. 7: Types of Drainage Network	28
Figure 3. 8: Age of houses	29
Figure 3. 9: Raw materials used for foundation	29
Figure 3. 10: Materials used for floors	30
Figure 3. 11: Materials used for Walls	31
Figure 3. 12: Roofing Materials	31
Figure 3. 13: Whether they have obtained any technical assistance	32
Figure 3. 14: Whether they have obtained a CoC	33
Figure 3. 15: Flood Heights	34
Figure 3. 16: Flood Duration	34
Figure 3. 17: Damages occurred to the components in building envelope	35
Figure 3. 18: Wall failed in flexure parallel to bed joint	36
Figure 3. 19: A collapsed and cracked wall	36
Figure 3. 20: Damages took place in the roof	37
Figure 3. 21: Damages occurred to the plaster board ceilings	37
Figure 3. 22: Damages emerged to the floor	38
Figure 3. 23: Loss of days of work due to flood	39
Figure 3. 24: Satisfaction with electricity	39
Figure 4. 1: Masonry Units	41
Figure 4. 2: Testing the compressive strength of masonry units	43
Figure 4. 3: Determination of initial rate of water absorption for FCB units	47

Figure 4. 4: Compacted mortar in the mold	51
Figure 4. 5: Condition of the mortar after removing the mold	51
Figure 4. 6: Mortar after jolting for 15 seconds	52
Figure 4. 7: Flexural Testing of a mortar prism	55
Figure 4. 8: Compression testing of a mortar prism	56
Figure 4. 9: Testing arrangement for water absorption coefficient of mortar prisms	56
Figure 4. 10: Geogrid	59
Figure 4. 11: PVC coated Welded Wire mesh	59
Figure 4. 12: Different variables introduced for wall panel construction	60
Figure 4. 13: Steps followed from construction to testing of wall panels	63
Figure 4. 14: Experimental Setup	64
Figure 4. 15: Variation of flexural strength parallel to bed joint for FCB wall panel	66
Figure 4. 16: Variation of flexural strength parallel to bed joint for CB wall panel	67
Figure 4. 17: Flexural strength increase in parallel to bed joint of retrofitted FCB wall panel	67
Figure 4. 18: Increase in flexural strength parallel to bed joint of retrofitted CB wall panel	68
Figure 4. 19: Percentage reduction of flexural strength of masonry wall panels from dry condition to saturated condition	69
Figure 4. 20: Observed failure patterns during the experimental program	72
Figure 5. 1: Front view of the model house	75
Figure 5. 2: Procedure of retrofitting with geogrid	76

## LIST OF TABLES

Table 2. 1: Actions to be considered in the context of flooding, source: Bowker et al., (2005).	10
Table 2. 2: Various retrofit configurations for masonry wall panels	18
Table 2. 3: Experimental results and comparison	18
Table 2. 4: Experimental Results	20
Table 3. 1: Areas and Number of houses utilized for the survey	24
Table 4. 1: Normalized compressive strength of FCB (oven dry condition)	44
Table 4. 2: Normalized compressive strength of the FCB (saturated condition)	44
Table 4. 3: Normalized compressive strength of the CB (oven dry condition)	45
Table 4. 4: Normalized compressive strength of the CB (saturated condition)	45
Table 4. 5: Initial rate of water absorption for FCB units	47
Table 4. 6: Initial rate of water absorption for CB units	48
Table 4. 7: Total water absorption for FCB units	48
Table 4. 8: Total water absorption for CB units	49
Table 4. 9: Summary of the properties of masonry units	49
Table 4. 10: Flow values of mortar used to cast and render with different conditions for FCB wall panels	53

Table 4. 11: Flow values of mortar used to cast and render with different conditions for CB wall panels	54
Table 4. 12: Physical properties of mortar used for FCB wall panels	57
Table 4. 13: Physical properties of mortar used for CB wall panels	58
Table 4. 14: Properties of wire mesh and geogrid	59
Table 4. 15: Average flexural strength parallel to bed joint of FCB wall panels	65
Table 4. 16: Average flexural strength parallel to bed joint of CB wall panels	65
Table 4. 17: Percentage increase of the flexural strength values compared with dry plain masonry	69
Table 4. 18: Cost per square meter of wall panel	73

# **1. INTRODUCTION**

## **1.1 Research background**

A profound and extreme climate and weather occasions which can be called as natural hazards become tragedies when people's lives and livelihood are disrupted. A remarkable amount of human lives and property all over the world is being lost due to these dreadful incidents. Among the regions in the world, Asia can be recognized as one of the most disaster susceptible regions as reported by Sung Eun et al., (2015). Since 1970 the region has been hit by more than five thousand natural disasters affecting the lives of more than six billion (Sung Eun et al., 2015). Higher frequency and intensity of extreme and severe events are being experienced due to the rapid transformation of global climate. Hurricanes, floods, earthquakes, landslides, extreme temperature and drought and tsunamis are some examples of natural disasters which can be encountered as a result of this considerable change in the climate (Win et al.,2018) and (Jamali et al., 2018). These calamities have left annihilation throughout the world with notable effects to both the economy and the social lives of those affected (Siriwardana et al., 2018). According to the Global risk report 2019, extreme weather events were ranked as the top risk out of ten risks in terms of likelihood and third in terms of impact.

Flooding, which is accountable for the second-highest fatalities in the region, according to the aforementioned report has created detrimental effects such as mortality, homeless people and widespread destruction of infrastructure and property (Dewan, 2015). It can be recognized as one of the greatest impacts of climate change conforming to Jamali et al., (2018). Many countries in the region have been affected severely due to the devastating floods and causes grievous impacts resulting in disturbances in transport, communication, significant negative impacts on the environment, intervention with the public services and downgrading the quality of water leading to substantial economic and social impacts (Jamali et al., 2018). In addition to that, it damages dwellings triggering short and long-term consequences for everyone who are affected (Kemi et al., 2017). China is one of the victims of floods which had spent more than US dollars 10 billion annually for flood damages and recorded more than thousand flood fatalities (Huang et al., 2019). Furthermore,

Bangladesh and Nepal which were located in the South Asia zone are two densely populated countries that encounter divergent varieties of floods every year with unfavorable impacts on their economy (Dewan, 2015). Sri Lanka was also encountered with a massive flood as a result of the tsunami in 2004 with a significant loss of human lives (Mendis et al., 2014). Furthermore, damages happened to the properties and the rehabilitation cost to be incurred can be identified as one of the major concerns after an event of flooding.

Hence flooding in various parts of the world is an ever-growing part of everyday life and the disasters firmly create problems for the people who lived in areas which are most vulnerable floods. The deprivation of low-income people in developing countries are made worse in extreme flooding events and create well generated problems linked to hydrological conditions, environmental deterioration as well as social inequality. The repercussions of these events under increasing pressure from urbanization and global environmental change would be declined if infrastructure, building techniques, and institutional support systems are improved with time.

## **1.2 Masonry Structures**

A significant portion of existing buildings around the world is consisted of unreinforced masonry structures. Mendis et al., (2014) declared that buildings can be separated into two main categories as engineered and non-engineered. Unreinforced Masonry (URM) structures which can be classified as non-engineered type is more than 70% of the buildings available globally (Matthys and Noland, 1989). These structures were utilized in most of the constructions due to its minimum need of skilled labours, durability, cost effectiveness, local availability of materials, constructability and Eco friendliness.

These structures are performing well under the gravity loading (load which acts in plane) because of their ability to withstand loads which are applied as compression. Anyhow, masonry structures do not behave well when they are undergone to lateral loads (out of plane loading) due to the deficiency of shear, tension and flexural resistance. Therefore, nearly all of the masonry structures have detrimental effects due to additional lateral loads induced by the flood. Hydrostatic, hydrodynamic and impact

loads can be identified as the additional lateral loads induced by the floods. Due to the ponding effect of flood water, the variation of water level on either side of the wall create a net lateral force (hydrostatic force) on the wall, which can cause significant deformation of URM walls.

Hydrodynamic forces can also take place due to velocity of the flooded water and the impact load which can be arisen from floating debris at flooding. Therefore, it has been found that the catastrophes occurred in URM buildings were caused because of out of plane failure of the URM walls (Reza Amiraslazadeh, 2012). It is vital to develop a suitable method that would improve the out of plane performance of masonry walls and time required for the collapse.

The concept of retrofitting the masonry structures can be identified as one such approach to enhance the out of plane behavior of the walls. Hence it will subsequently prevent the unexpected collapse of walls during natural hazards and allows people to evacuate safely (Bartolome et al., 2014). It should be noted that demolishing or rebuilding the existing structures would undergo more cost and investment on natural resources and may not be upholding to a sustainable built environment. Therefore, it is predominantly important to find an appropriate retrofitting method to reinforce the URM walls against natural disasters.

Several conventional retrofitting methods have been developed and discovered to improve lateral strength of the masonry walls such as surface treatment (ferrocement, shotcrete), grout injection, external reinforcement etc. Researchers have identified the advantages and also the disadvantages of these techniques. This study has been focused mainly to identify suitable retrofitting techniques for local context.

It could be noted that URM walls can be damaged by two potential failure methods, namely in plane and out of plane (El Gawady et al., 2006). Most of the researches have been carried out to enhance the strength of URM walls subjected to in-plane loading. Hence the study presented here has been focused on the out of plane loading in masonry walls exerted by flooding. URM walls can be failed in flexure parallel to bed joint or flexure perpendicular to bed joint when exposed to an out of plane loading.

A field survey of the houses damaged due to floods was carried out as the initial part of this study in flood-affected areas of Sri Lanka (Kalutara, Galle and Matara) to identify the gravity of the effects due to flooding. Most of the damaged structures due to the floods were domestic URM dwellings made out of FCB and CB.

One of the main observations during the field survey was recurrent nature of the failure mechanism due to floods, which can be recognized as the flexure parallel to bed joint of URM walls. Therefore, the main objective of this experimental program was to improve the flexural strength parallel to the bed joint of URM walls.

### **1.3 Objective**

The main objective is to develop a feasible retrofitting system for low rise masonry structures to withstand the adverse forces of nature.

### **1.4 Methodology**

- Possible failure mechanisms of low-rise masonry structures due to flooding were analyzed and the most predominant building element damaged was also identified.
- Different types of retrofitting methods and materials were identified based on a detailed literature review.
- Tensile strengths of Geo grid and wire mesh were determined as a mechanical property.
- Two types of commonly used masonry materials; FCB and CB were used in wall panel casting for the entire experimental program.
- The experimental program consisted of testing the unit strength and determining the water absorption coefficient of masonry units and flexural strength parallel to bed joint (BS EN 1015-2) with and without retrofitting for both dry and saturated conditions.
- Analyze the results of the experimental program and selected the most suitable retrofitting type.
- A brief cost study was carried out based on the experimental program and the practical application of the outcome to a house affected by floods.



## **1.5 Arrangement of the thesis**

In this report the research project has been presented under six chapters. The first chapter contains the introduction, background, problem identification, objectives and methodology of the research.

Second chapter contains the details of past research studies done locally and globally relevant to the proposed research title and the research gap.

Third chapter contains about the field study while the fourth chapter discusses the experimental study.

Then, the fifth chapter contains about the practical application of the experimental study.

Final chapter contains the conclusions and suggestions for future work relevant to the research topic.

## 2. LITERATURE REVIEW

### 2.1 Introduction

In order to formulate better risk reduction approaches, flood risk assessment can be considered as a vital tool. Assessing the damages occurred due to flooding is one of the key components in flood risk assessment. Some research was carried out to find the damages occurred after an event of a disaster. However, it is important to work on flood resistance at an early stage by accumulating and exploring data from field surveys and thereafter to propose suitable methodologies to confirm the safety of dwellings against flooding and to improve the capacity of flood resilience. This research was based on the key findings discovered from a field survey as stated below.

Furthermore, a considerable amount of research regarding the performance of unreinforced masonry (URM) structures under lateral loading has been executed locally and globally as stated in Figure 2.1. However, there are limited studies carried out on out of plane loading of walls and occasionally very few have explored the combination of out of plane loading and saturated condition. In this chapter, above-mentioned research tasks have been considered to obtain a satisfactory understanding about the existing findings relevant to URM structures.

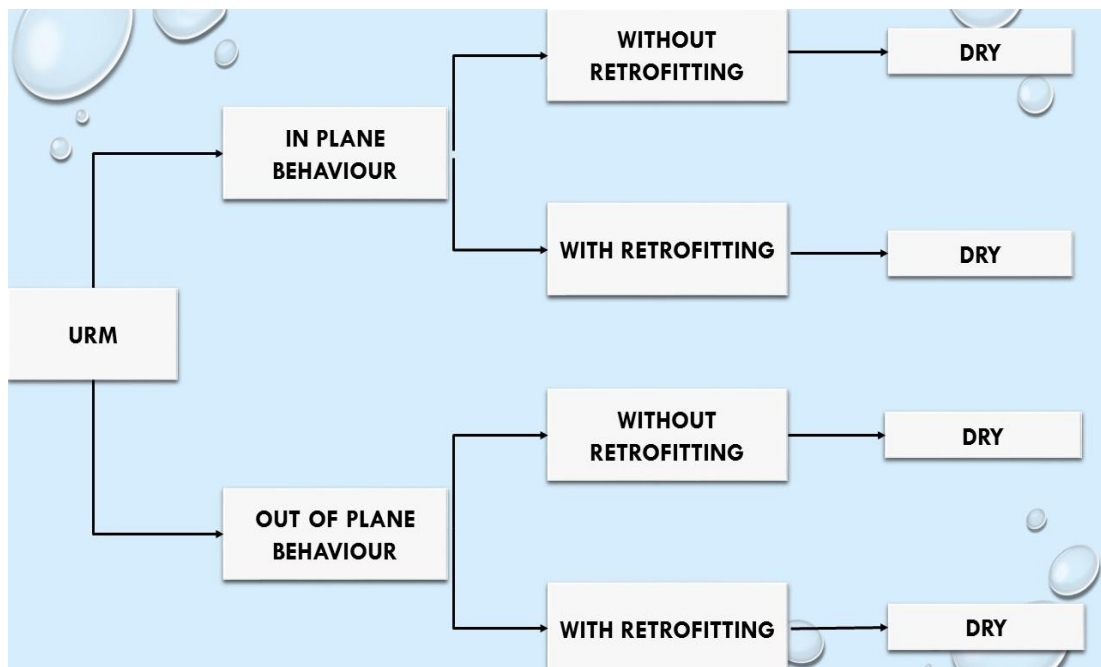


Figure 2. 1: Prevailing studies relevant to masonry structures

## **2.2 Investigate the magnitude and the nature of the damage, types of structures affected, impact on human lives in post disaster stage**

Despite considerable research on how to resist this natural calamity and the actions taking place for more resilient structures, a clearer proportion of existing construction techniques are still inappropriate for the risk of flooding (Kemi et al 2018).

Hence mitigation and preparedness under the pre-disaster phase are high leading to insufficient and then response and recovery under the post disaster phase become more expensive and time consuming. Therefore, the necessity of proper preventive and protective measures has been raised to mitigate the harmful impact of a flood event on physical, social and economic components in future.

Flood risk assessment which can be considered as essential for disaster preparation and the results which were obtained from it are paramount importance for policy makers with vital tools for formulating better risk reduction approaches. Assessing the damages occurred due to flooding is one of the key components in flood risk assessment. A questionnaire survey for past damages can be identified as a technique to estimate the damage in future floods since it has been accepted to be the most reliable way to predict the flood damage. These surveys can be a tremendous value for evaluating the risk of future damages. Depth and the duration of flood have been identified as most suitable variants for destruction caused by flooding (Win et al., 2018).

According to literature, the damage functions for flood risk assessment in Colombo, the relationship between disaster risk, poverty and household vulnerability in North Central Province in Sri Lanka have been already observed and developed by Dias et al., (2018) and Silva et al., (2018) respectively. Using questionnaires, in – depth interviews and focused group discussions Abeykoon et al., (2018) observed how the social cohesion emerges in Sri Lanka after a sudden disaster and how it is helpful to rebuild affected people's life.

Worldwide, Behera et al., (2018) assessed household vulnerability and adaptive capacity in a flood prone area of the Eastern Indian State of West Bengal. The instability on the slopes and along the streams during a flood event were observed

through field surveys by Luino et al., 2018) for two severe floods occurred in the Upper Soan Valley.

A face to face survey to determine three key flood preparedness efforts taken by occupants in ten poor communities were assessed by Atreya et al., (2017).

In Pakistan, Mahmood et al., (2016) determined the physical and economic damages resulted by a flash flood in 2010 based on questionnaires and GPS survey. Further, Qasim et al., (2016) surveyed the community resilience to flood hazards in terms of social, economic, physical and institutional and found that the resilience can be enhanced through awareness, preparedness and structural and non-structural measures. Additionally, Ali et al., (2015) carried out a structured questionnaire to investigate risks related to climate change and adopt measures used by Pakistan farmers to avoid adverse impacts of natural disasters.

Lamprey et al., (2017) emphasized on evaluation and plotting of social flood risk in the Lower Mono River Basin, West Africa and Shubham et al., (2018) aimed at learning from the experiences of women entrepreneurs who went through 2011 floods in Thailand by key interviews, questionnaire surveys and focus group discussions.

Following similar procedures discussed in above mentioned studies, a comprehensive field survey was carried out in severely affected areas due to recent floods with the aim of learning from those experiences.

### **2.3 Unreinforced Masonry (URM) structures**

Unreinforced masonry (URM) construction is one of the oldest forms of construction and today comprise one of the largest sectors of decaying building stock in every quarter including industrial, residential, and even historic monuments. The need to update or retrofit these structures is undeniable and urgent since failures of these structures in the ever-increasing presence of natural disasters are responsible for a majority of fatalities during those events (Papanicolaoa, et al., 2011).

URM buildings contains a noteworthy portion of existing buildings around the world according to El Gawady et al., (2005). It was revealed that the buildings could separate into two major sections as engineered and non-engineered. The greatest number of

URM around the world can be classified as non-engineered that is assessed to 70% of the total [Mendis et al., 2014]. These structures were employed in most of the construction due to its need for less skilled laborers, durability, low cost, Eco-friendliness and can be built with locally available materials.

URM buildings can be mainly classified into three forms based on its constituents; bricks, stone masonry and adobe. Each of these, is dependent on availability of materials, geographic location and level of construction knowledge or experience of that area. URM structures are the dominant form of construction in rural areas of developing countries in particular where the population is generally comprised of low-income people with limited knowledge of construction or engineering practices (Bhattacharya 2014).

### **2.3.1 Forces acting on URM walls**

Horizontal (Lateral) and vertical loads are the two categories of loads acting on masonry walls in terms of the direction. Dead load and imposed load can be included as vertical forces and wind loads, earthquake loads, impact loads, hydrostatic and hydrodynamic loads due to flooding can be grouped as the horizontal loads (Seron & Suhoothi, 2017). URM walls are predominantly damaged as a flexural failure by the lateral loads in an event of a flood due to its poor flexural capacity. Net lateral forces may become consequential to cause a deformation of the URM wall due to a considerable difference of around 1 m-1.5 m in water levels present on opposite sides of the wall (Kelman & Spence, 2003).

Furthermore, hydrodynamic forces are capable of damaging structural masonry walls which are functions of floodwater velocity and building geometry. Impact loads which can be emerged from coastal flooding and floating debris could be more destructive than hydrodynamic and hydrostatic loads. Those that have been discovered, deficit a cohesive approach in acquiring and scrutinizing data since due to the fact that events such as these are highly changeable and strenuous to put into an analytical model. Some of the variables to consider have been summarized by Bowker et al. (2005) and shown in Table 2.1.

Table 2. 1: Actions to be considered in the context of flooding

Source: Bowker et al., (2005)

Actions	Impact on the structure
Hydrostatic	Outcome of the hydrostatic pressure acting on the building either through lateral or uplift forces imposed by the nearby flood waters and saturated ground.
Hydrodynamic	Hydrodynamic forces generated by flowing water surrounding a building which increase with rising flood depth and velocity.
Debris	The collision of another object against the building, either static or dynamic, such as an object being propelled into the building.
Non-physical	When the building materials are affected by the chemical composition of the water such as in the case with saltwater or sewage or after the flood.
Direct water	Building material performance may be impacted due to direct contact with the water through swelling or dissolution.

It should also be highlighted that these variables are not mutually exclusive and in fact may compound each other. Ultimately, it is suggested that the most unfavourable effects relating to flood damage are the lateral hydrostatic forces, lateral hydrodynamic forces and direct water contact.

### 2.3.2 Out of plane behavior of masonry walls

Although research on masonry construction comes from early twentieth century, there remains a great variation in the results of previous and current studies. This is in part due to the high variability of the material itself and also due to the imparted variance by human involvement during manufacturing and construction (Abdellate 2011).

There are few numbers of studies carried out on out of plane loading of walls by Dizzhur et al., (2014), Faella et al., (2010), Hamed & Rabinovitch (2010), and Gilstrap & Dolan (1998) or the performance of construction materials during flood events (Ingargiola & Moline 2013, Ghissi et al., 2013, and Herbert et al., 2012) and occasionally a hand full of researches have investigated the blend of out of plane loading and saturated conditions. Dizzhur et al., (2014) performed a laboratory based experimental program by replicating the attributes of URM discovered in historic

masonry buildings. In this study, the out of plane performance of masonry walls was improved by investigating the performance of near surface mounted (NSM) carbon fiber reinforced polymer (CFRP). The most favorable CFRP piece and the shape of the groove were chosen depending on the results acquired from an experiment in pull-out strength. Furthermore, a validation with the design methodology was carried out by an experimental program.

In the aforementioned study that was done by Dizzhur et al., (2014), nine masonry beams and five full scale masonry walls were cast and tested which consist a mortar mix of 1:2:6 (Ordinary Portland Cement, Hydrated Lime, Sand) and 1:2:9 respectively. The walls were built with a thickness of two and three leaves and a bed joint thickness in between 10mm to 15mm. These walls were cured for 28 days before applying the bonded CFRP strips. Figure 2.2 presents the arrangement of necessary equipment and the test specimen which was used during the experiment.



*Figure 2. 2: Arrangement for the testing*

So, the test results from that previously carried out study revealed use of vertically oriented CFRP strips that were placed in a vertical direction in the aforementioned

masonry walls outstandingly improved the post cracking wall strength in between 3.05 to 6.21 times of the as built wall strength as well as the ductility.

The aforementioned study further revealed that Near Surface Mounted (NSM) CFRP retrofit technique provides an uncomplicated replacement to URM buildings and their components by considerably improving their out of plane behavior when subjected to seismic loads. The authors recommended that this method has a negligible influence on the appealing nature of the retrofitted building.

Hamed and Rabinovitch (2010) executed an experimental program to identify the failure characteristics of Fiber Reinforced Polymer (FRP) strengthened masonry walls under out of plane loading. Two full scale walls (a control specimen and a wall reinforced with FRP strips) were built and loaded up to failure. Figure 2.3 expresses the structural performance of stiffened masonry wall with FRP which is subjected to out of plane loading.

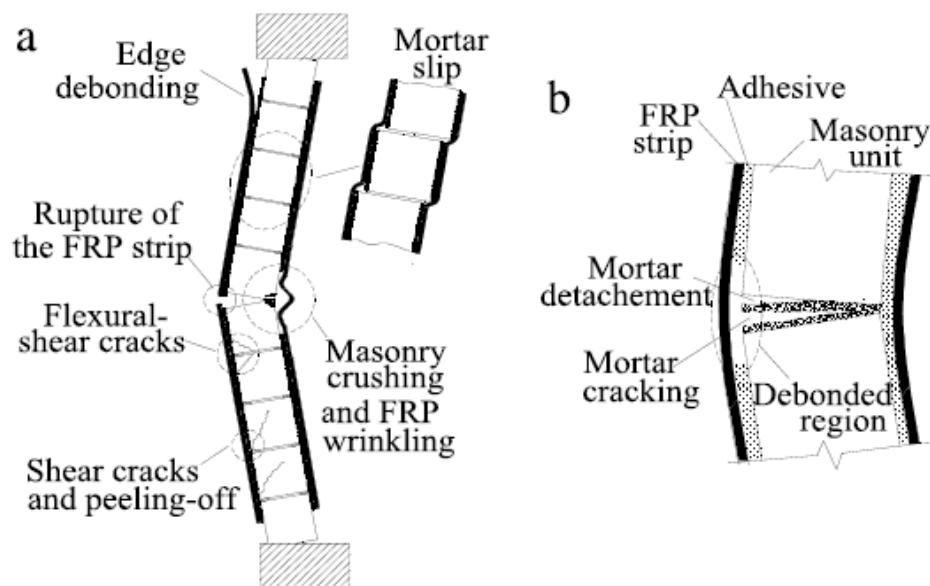


*Figure 2. 3: Structural functioning of reinforced masonry wall subjected to loading (out-of-plane)*

The experimental study that was done by Hamed and Rabinovitch (2010) was carried out under two phases. Phase one was mainly focused on characterization of constitutive behavior, mechanical properties of different materials, elements and interfaces used for the experiments following with determination of various



parameters used in the experimental program. Furthermore, producer's data sheet was utilized to obtain some material properties. A full-size masonry wall reinforced with surface glued composite CFRP strips and an unreinforced control wall were subjected to out of plane forces as the second phase. The control wall was failed with observations such as fragile and sudden while the failure of the reinforced wall was occurred as a consequence of shear failure in masonry units related with de bonding of the CFRP. However, it was observed that the strengthening process prevents the integrity and stability of the wall at failure. Figure 2.4 displays failure of the wall panel retrofitted with CFRP.

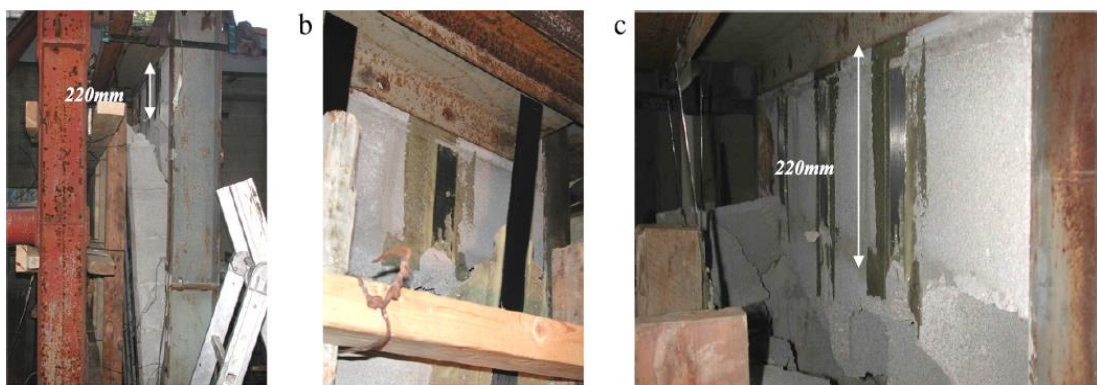


*Figure 2. 4: Failure of the reinforced wall due to shear*

In that study a notable observation was that the failure by shear or debonding is uncertain at free edges of CFRP strips on the reinforced wall with the CFRP. However, delamination of CFRP (material fracture into layers) was observed as the de bonding failure in other regions of the wall. The outcomes of the experiments have illustrated that under actual supporting circumstances, the effectiveness of the strengthening system is much lower than the efficiency factors specified in other past studies commonly for simply supported masonry walls.

Herbert et al., (2012) investigated the flexural strength of URM walls due to loading arise from flood water. An experimental program was implemented to evaluate the consequence of load applied due to hydrostatic pressure to the structure of the building in order to represent the lateral forces acting from floods. Masonry wall panels made out of FCB and autoclaved aerated concrete block units were erected at small scale (1/6<sup>th</sup>) and subsequently an out of plane hydraulic load has been exerted gradually until

failure happened. As stated by the authors, scaled down modelling of masonry has been utilized well by numerous researches and it permits testing to be accomplished cost effectively and cautiously. Testing arrangement of the wall panels is shown in Figure 2.5.

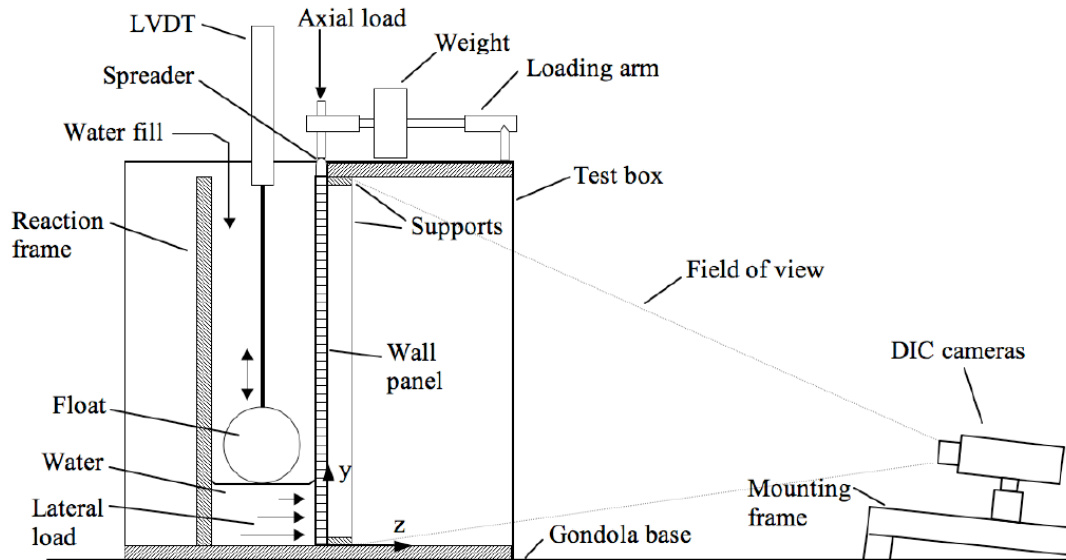


*Figure 2. 5: Testing arrangement of the wall panels*

Horizontal and diagonal cracks were noticed in panels just prior to final failure. Load deflection response was also monitored throughout the experiment.

The utilization of a Geotechnical centrifuge has accounted for the effect from self-weight of the wall panel hence correctly scaled to that of the prototype. Digital Image Correlation (DIC) study has allowed to investigate the mechanism of crack development than previously available studies with the aid of both discrete points and surfaces. 1.05 m and 1.25 m were the water levels that were recorded at failure for specimens made out of Autoclaved aerated concrete (AAC) units and FCB units respectively.

Flood damage in Sri Lanka can be classified to floods with respect to the source such as, riverine, flash, regional, and floods generated by reservoir functioning or breaking. All of these possibly will happen within the same event and are repeatedly accountable for substantial damage with intensifying recurrence as declared by the “Sri Lanka National Report on Disaster Risk, Poverty and Human Development Relationship” (2009).

An outline of disaster events in Sri Lanka has been identified based on the Sri Lanka historical disaster information system by the Disaster Management Centre (DMC) (2009) and summarized in Figures 2.6 and 2.7 describing the impact on residences in Sri Lanka over time without the 2004 tsunami.

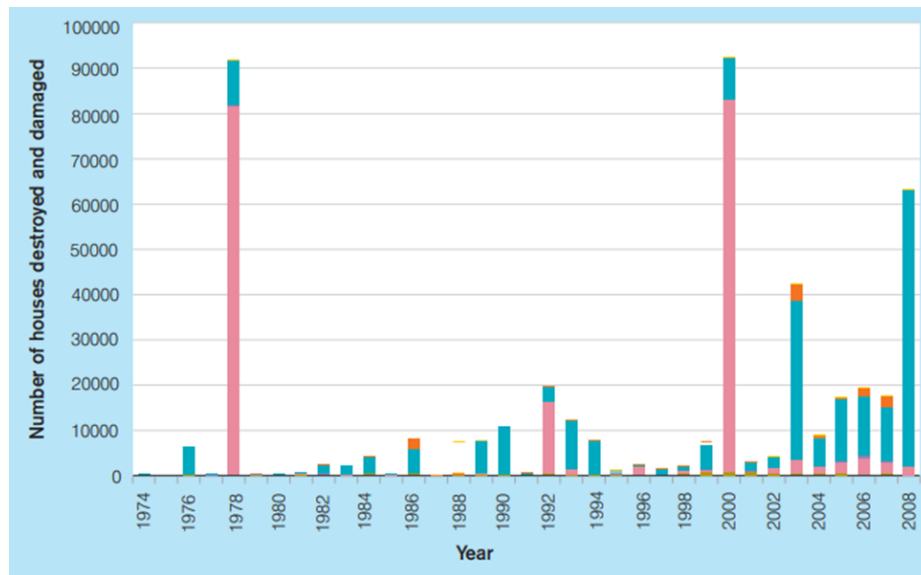


Figure 2. 6: Annual time series for damaged or destroyed houses in Sri Lanka due to disasters (excluding Tsunami)

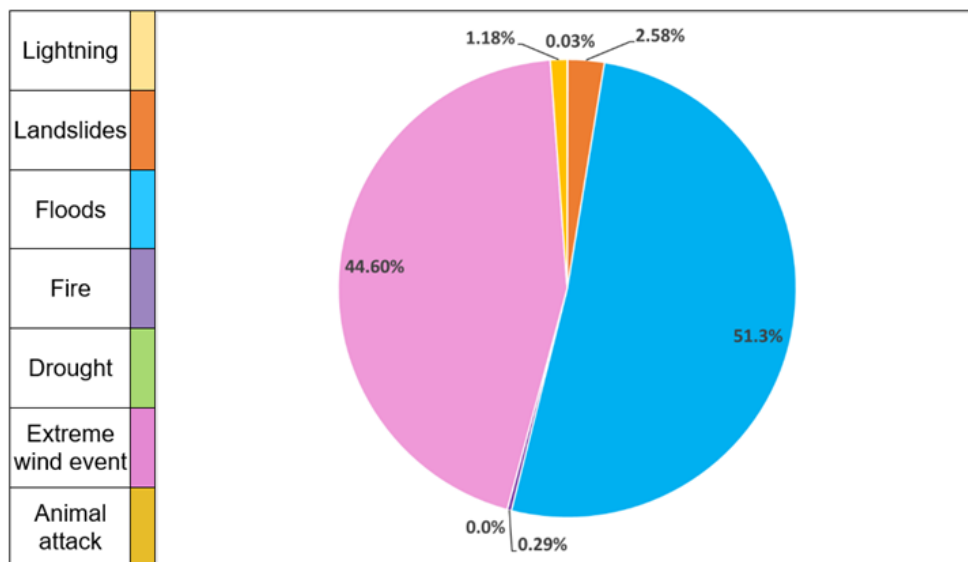


Figure 2. 7: Profile of houses destroyed and damaged due to disasters excluding tsunami: 1974 -2008

As the danger created by exposure to flooding increases, the need for research also increases. It is evident from previous studies that the calamities occurred in URM

buildings were caused because of the out of plane flexural failure of the URM walls (Amiraslanzadeh et al., 2012).

An appropriate technique should be deployed to improve the out of plane behavior of the walls. Thus, it will eventually prevent the sudden collapse of walls during natural hazards and let people to evacuate safely (Bartolome et al., 2004). It should be noted that dismantling or rebuilding the existing walls would spend excessive cost on natural resources and hence may not be satisfying to match with the sustainable built environment. Therefore, it is absolutely necessary to find a suitable method to strengthen the URM structures against natural disasters. Retrofitting of masonry walls has been found as a probable answer to strengthen the masonry structures against lateral loads occurred from natural hazards (Bui et al., 2015).

### **2.3.3 Retrofitting of URM Structures**

There are some investigations that have been carried out on the structural strengthening of both reinforced and URM construction [Drysdale & Khattab (1995), Luccioni & Rougier (1995), Bhattacharya et al. (2014)] and most of these have been narrowed to in-plane loading with a focus on seismic conditions.

Bernat et al., (2013) conducted a testing program by applying an eccentric compressive loading on real size masonry walls strengthened with textile. An experimental study for the Static cyclic test was done to investigate the in-plane behavior of URM walls retrofitted with shotcrete (ElGawady et al., 2006).

Blondet et al., (2006) carried out a study that applied two kinds of polymer mesh which were a mesh with weaker mechanical properties that is conventionally utilized as a 'soft' barricade on building sites and a commercially utilized Geo-grid.

In this study, the wall was covered with the mesh in key locations and then overlaid with a mud plaster finish. Each one of the specimens was dynamically tested for in plane loading with the aid of an uni- directional shake table. Half scale URM walls that were confined with reinforced concrete ties were subjected to in plane cyclic loading by Paikara et al.,(2006). The experiments signified that restraining wall

segment into little components upgrade the dissipation of energy and in-plane deformability of the walls.

Seismic wallpaper or glass fiber-reinforced polymer (GFRP) reinforcement was used on numerous specimens of URM walls with solid clay brick and low strength mortar. All the walls were retrofitted with vertical composite strips which were bonded on both sides of the wall by applying epoxy resin. Loading in lateral direction and displacement using a loading system of air bag was applied to each wall specimen. It was found that the pressure inserted to all retrofitted wall samples was improved by 10 to 32 times of the weight per unit surface area of wall panels hence improving the ultimate flexural strength (Ehsani et al., 1999).

Bischof & Suter (2014) performed a comprehensive analysis by embedding carbon meshes to a specially developed mortar. The selected mortar was an outcome comprised of fibers, inorganic binders, polymers and selected aggregates.

The surface was cleaned by using pressurized water and then a mortar layer was sprayed and then the carbon mesh was positioned on it using mechanical anchorage and it is of paramount importance to orientate entire carbon fiber of the mesh.

After that, the second layer of mortar was applied until the overall thickness of the retrofitting was about between 15mm and 25mm. If require, carbon meshes can be placed as two layers resulting in thickness within the range of 25mm and 35mm. Aluminum profile was used to anchor the carbon mesh to the wall. An experimental program was implemented for different test specimens which were constructed with various retrofit configurations are in Table 2.2.

The static-cyclic load test was performed on retrofitted masonry walls for the determination of the performance of this novel strengthening system. Loads were applied on the wall panels by using a specifically designed test set up. Figure 2.8 elaborates on the arrangement for the cyclic static load test. In the aforementioned test, both lateral and in plane forces were applied at the same time.

Table 2. 2: Various retrofit configurations for masonry wall panels

Specimen No	Retrofit Configuration
1	Reference wall (No retrofitting)
2	Carbon mesh strips that was applied vertically (2 Nos)
3	Two Carbon mesh strips applied vertically and diagonally (45°)
4	Two and four, applied carbon mesh strips vertically and diagonally (45°) respectively
5	Two and four, applied carbon mesh strips vertically and diagonally (60°) respectively

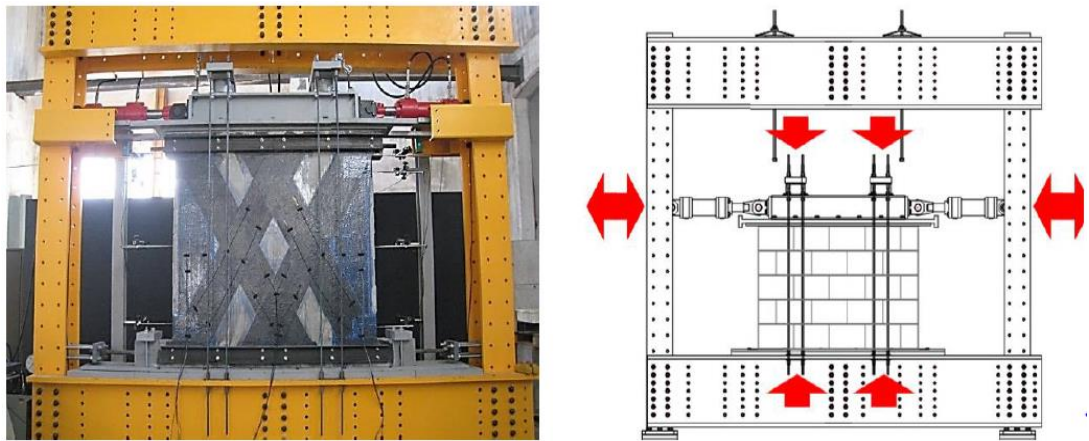


Figure 2. 8: Arrangement for the experimental program

Furthermore, in - plane behavior of the walls was tested throughout this study. The maximum horizontal load applied to each specimen and the displacement was recorded. The results are presented in Table 2.3.

Table 2. 3: Experimental results and comparison

Specimen No	Maximum horizontal load (KN)	Comparison to the reference wall	Maximum displacement (mm)	Comparison to the reference wall
1	75.2	100%	10.1	100%
2	110	145%	14.5	138%
3	109	147%	11.8	111%
4	120	159%	12.2	119%
5	121	161%	11.2	108%

The maximum load carried by each wall has increased due to retrofitting of wall specimens with coated carbon mesh. It has been recorded that the ultimate horizontal force gained by the wall specimen MR-C5 was increased up to 161% comparing to the reference wall. Furthermore, the ultimate deformability of wall panels was observed about 138% of the deformability of the reference wall. It can be concluded that the lateral load carrying capacity of the masonry wall specimens has been increased by introducing the aforementioned retrofitting technique.

Macabuag et al., (2012) introduced a seismic retrofitting method for non-engineered masonry houses in Nepal. The study was aimed to introduce a retrofitting technique for preventing and prolonging the collapse of the adobe houses under strong earthquakes. PP (Polypropylene) packaging straps were used as the retrofitting material. The authors suggested using this method for low-income houses. A mesh was formed by arranging the individual PP bands into a grid and electrically welding at intersecting points. Wall panels were cast at a linear scale of 1:4 and the PP bands were 12 mm wide and 0.4 mm thick. An anchor beam at floor level and a ring beam at the top level of the wall panels were constructed and the mesh was fixed to the wall by drilling through it to the beams and the wall panel using ties. The mesh was fixed to both faces of the wall panels and both meshes were connected by using wires and pre-drilled holes through the walls. Finally, the mesh was covered by using a mortar to protect it from sunlight, to avoid the visibility of the mesh to the outside and to increase the fixity of mesh to the wall.

The static loading test was done to evaluate the performance of the retrofitted wall panels. Shear resistance of the wall specimens for in-plane lateral load was determined through this test. The initial failure load was unaffected by the presence of the mesh. However, non-retrofitted walls were subjected to a brittle failure with no further load maintained whereas retrofitted specimens were continued to maintain the load after initial failure.

According to the results obtained from the aforementioned study retrofitting of masonry walls by using PP mesh enhanced the safety of existing masonry building in earthquakes. Furthermore, the structural integrity of walls is being sustained for a

considerable amount of time before the total failure during the earthquakes therefore people will be able to evacuate from the houses safely with their belongings.

An experimental study was conducted by Mansourikia and Hoback, (2014) to identify the performance of masonry retrofitted with Geotextile and carbon fiber reinforced polymer (CFRP). Ten specimens of unreinforced masonry walls were constructed by using hollow concrete blocks and connecting them with 12 mm thick grout. The height and width of the specimens were 1100 mm and 1060 mm respectively. The retrofitting materials were bonded to the wall specimens with Epoxy which was applied along the length of the reinforcing strip. Both geotextile and CFRP strips were placed in a crossing pattern from corner to corner on the wall. Tests were conducted with hydraulic ram vibrator assemblies and the force and displacement were obtained through a data logger. The maximum amount of time spent before the failure of the wall specimens was recorded. Table 2.4 presents the Experimental results of the aforementioned test.

Table 2. 4: Experimental Results

<b>Retrofitting material</b>	<b>Width of the strip (mm)</b>	<b>Maximum time spent before failure (s)</b>
No retrofitting	0	65
CFRP	100	119
Geotextile	100	92.5
CFRP	200	157
Geotextile	200	112.5

A notable observation was that the retrofitting of masonry wall panels has increased the time spent before the failure. However, the wall panel retrofitted with CFRP has shown a higher failure time than that of Geotextile. But a comparable performance has been shown from the wall retrofitted with geotextile comparing to the reference wall. According to the authors commercially available CFRP is about 20 times more expensive than the geotextile. Hence using geotextile is more economical than CFRP and is manufactured widely across the world. Therefore, in this study, the geotextile



was suggested as a potential retrofitting material than CFRP. Figure 2.9 exhibits the test apparatus with CFRP applied to wall.



*Figure 2. 9: Test apparatus with CFRP applied to wall*

## **2.4 Summary**

Floods can be considered as one of the natural hazards which cause detrimental effects on the survival of mankind. Most of the fatalities have occurred due to damages in masonry walls of unreinforced masonry structures. These walls have failed due to their lack of capacity to resist lateral forces exerted by floods. Retrofitting of masonry walls has been identified as a potential solution to strengthen the masonry structures against the aforementioned forces. Many of the researches have been done in the past to strengthen the masonry walls by using different retrofitting types.

However, most of them are limited only to in plane performance of walls with retrofitting. The study presented here has focused on the lateral loads exerted by flooding. The commonly occurring failure mechanism due to floods has identified as the flexure parallel to the bed joint of the masonry walls based on a field study conducted in the flood affected areas of Sri Lanka. Therefore, the experimental program was mainly focused on flexure parallel to bed joint with a bed joint thickness of 17.5 mm. FCB and CB were used as the walling material for panels whereas geogrid and wire mesh were used as the retrofitting materials for the research. Furthermore, a brief cost study was carried out based on the experimental program for retrofitting of 1m<sup>2</sup> of masonry wall.

### **3. FIELD STUDY**

#### **3.1 Introduction**

This section describes about the field study which was carried out in flood affected areas and the key findings from it.

#### **3.2 Field Survey**

In order to carry out a comprehensive field study the most recent, 2017 flood, resulted during the southwest – monsoon was selected. According to Sri Lanka rapid post disaster needs assessment report, in 2017 flood, heavy rains ranging from 406 mm to 619 mm were received within 12 hours in the southwest region. There were 15 districts affected by flood reporting 212 deaths and 717,622 affected people as a result of this calamity. Furthermore, around 2313 houses were completely destroyed while 12,529 houses were partially damaged. According to the British Broadcasting Corporation (BBC), Figure 3.1 presents the severity of the flood event occurred in Kalutara district in the year 2017.



*Figure 3. 1: 2017 Flood level in Kalutara district, Source: BBC*

#### **3.3 Study Area**

According to the flood maps developed by the National Building Research Organization (NBRO) and Disaster Management Center (DMC), eight divisions which belong to Kalutara, Matara and Galle districts were selected as the study area.

These include Bulathsinghala, Dodangoda, Govinna, Neluwa, Thawalama, Athuraliya, Malimbada and Akuressa as indicated in the Sri Lankan map shown in Figure 3.2.



Figure 3. 2: Survey Locations

According to the 2012 Census data, the population of Kalutara, Matara and Galle districts were 1,221,948, 814,048 and 1,063,334, respectively. The population of three districts provided a total of 3,099,330. In order to calculate the sample size, Yamane formula (Equation. 1) was used that evaluates the value around 280. Subsequently, the proportional samples for Kalutara, Matara and Galle were 110, 74 and 96 respectively. These values have marginally complied with the number of surveyed houses.

$$n = \frac{N}{(1+Ne^2)} \quad \text{Equation 1}$$

Where;

n = Required sample size

N = Population size

e = Margin of Error (0.06)

### 3.4 Data Collection and Survey Format

The data were collected through questionnaires with the assistance of interviewers comprised of graduate engineers appointed by the Department of Civil engineering, University of Moratuwa. Table 3.1 presents the areas and number of houses which were examined and recorded during the survey.

Table 3. 1: Areas and Number of houses utilized for the survey

<b>DISTRICT</b>	<b>DIVISION</b>	<b>NO OF HOUSES</b>
Kalutara	Bulathsinghala	57
	Dodangoda	30
	Govinna	19
Galle	Neluwa	43
	Thawalama	37
Matara	Malimbada	43
	Akuressa	21
	Athuraliya	03
Total number of houses		253

Two sets of questionnaires were used in this study as the pilot and full-scale survey. Most of the time, household heads were interviewed, but in the absence of the household head, one of the senior family members was interviewed. A duration of 20-25 min was consumed for the completion of a single questionnaire. After documenting opinions and first-hand experience of the occupants, the structural defects were recorded by observation. Furthermore, physical measurements such as evidences of flood heights and flood duration with the motive of finding the saturation time were also recorded. In addition to that, the team was able to detect the indications of flood levels in some of the houses. This was followed by preparing excel sheets with the data collected as inputs with subsequent analysis focusing on damages due to the flood.

As the main attributes of the survey, details of the houses like age, compliance with the government approvals, building materials used and other related construction details were also considered. To determine the severity of the flood the height, duration and damages occurred due to flood were recorded and observed by the interviewers in the flood affected houses. This questionnaire survey has been expanded to measure the socioeconomic impacts by exploring the data related to loss of days to work and school and satisfaction with services such as water supply, electricity and transport.

Figure 3.3 elaborates different attributes of the survey such as land details, house details, government approvals, physical and socioeconomic impacts.

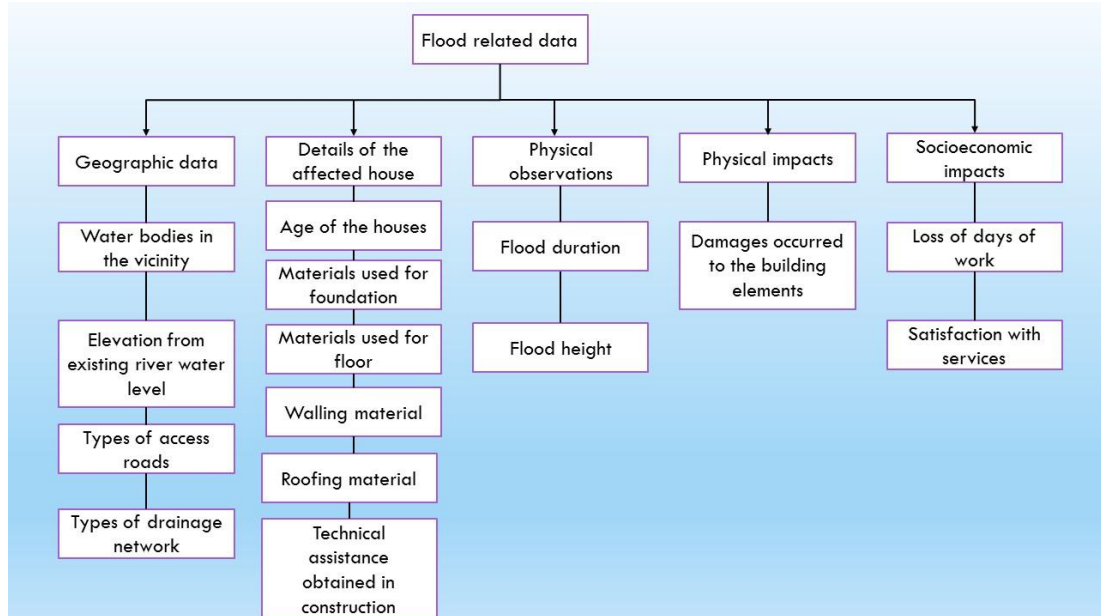


Figure 3. 3: Different attributes of the survey

### 3.5 Analysis of results

A detailed analysis of survey results was carried out based on the sub themes indicated in Figure 3.3. The results are presented in Sections 3.5.1 to 3.5.6.

#### 3.5.1 Geographic Data

Details of the lands affected by the flood were investigated under the aforementioned attribute.

##### 3.5.1.1 Distance to the closest body of water

All the houses surveyed in Matara, Kalutara and Galle districts were located on either side of the major river banks. In Matara district, the Nilwala river starts from the streams of the Gongala Mountain from the right bank of the Sinharaja Hill. It covers an area of about 81 km and the water level of the area is 960 sq. km.

Kalu ganga a river flows through Kalutara district with a length of 129 km, the river originates from Sri Paadhaya and reaches the sea at Kalutara. The river gets water mostly from the nearby range of mountains and the forest Sinharaja.

The Gin Ganga that is located in Galle district receive its water mainly from the mountains in Gongala area in Deniyaya. It flows past the villages of Neluwa and Thawalama.

As a result of heavy rain, the aforementioned rivers overflow and submerge lands nearby, creating significant problems for the residents. Figure 3.4 shows the percentage of affected houses that are within the distance of 1 km and more than 1 km to the closest body of water (a river) in each surveyed district.

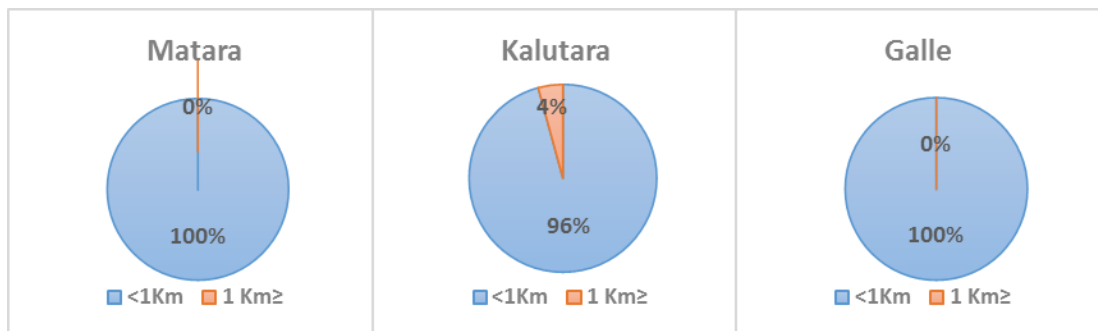


*Figure 3. 4: Percentage of houses which are within the distance of 1 km and more than 1 km to the closest body of water*

According to Figure 3.4, almost all the surveyed dwellings are within a distance of 1 km from water bodies hence these houses are vulnerable to damages that occurred by flooding. It is noteworthy to mention that flood was not severely affected to houses located a distance greater than 1 km.

### **3.5.1.2. Estimated elevation from river water level under normal flow condition**

This elevation difference is an important parameter since it decides the severity and the proportion of inundated areas submerged due to flooding. Figure 3.5 illustrates the percentage of houses indicating the estimated elevations (ft) from the river water level.

According to the Figure 3.5, 83 percent of the houses located at Matara and more than 50 percent at Kalutara are less than five feet in elevation from the river water level. Most of the adobes in Galle are located higher than ten feet in elevation when compared with houses located in Matara and Kalutara.

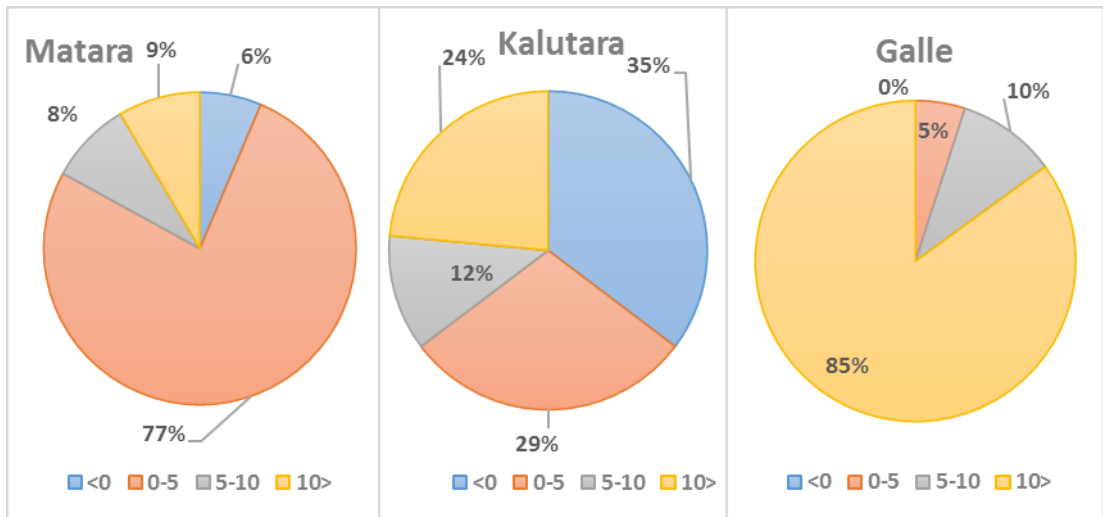


Figure 3. 5: Elevation from river water level (in ft)

### 3.5.1.3. Types of Access Roads

Access roads can be considered as one of the important geographical features since it is an evacuation path prior to and during an event of a flood. In order to provide relief to the flood affected communities by the rescue and relief teams, it is vital that the condition of the road after a flood should not be changed significantly (less eroded due to flooding). Figure 3.6 demonstrates the types of access roads and the percentage of houses in the regions of the survey.

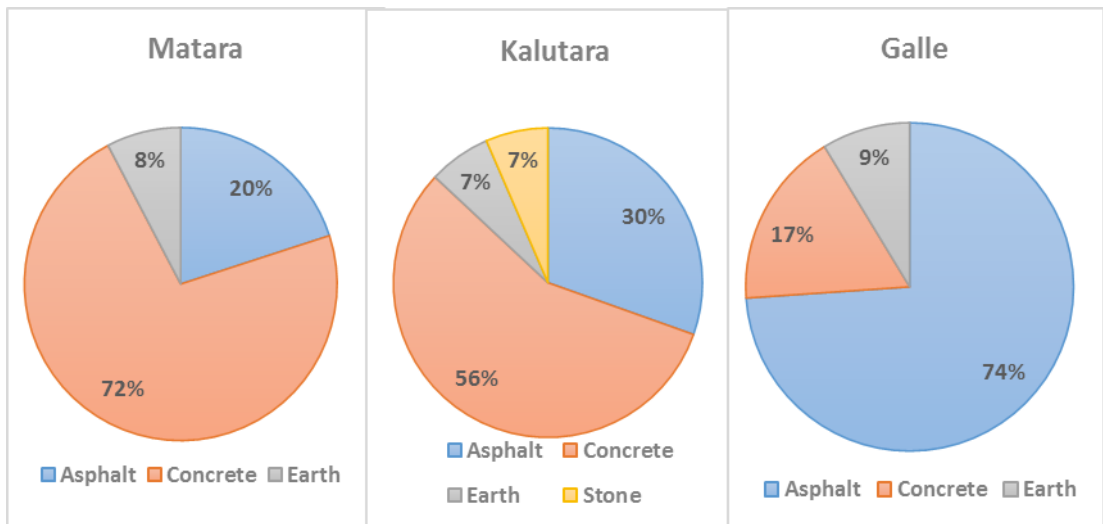


Figure 3. 6: Types of access roads

As stated above, concrete roads are identified as the most common type of road in Matara and Kalutara districts, whereas, in Galle asphalt roads can be recognized as the foremost type of access road.

### 3.5.1.4. Types of the drainage network

Lack of drainage infrastructure and failure to maintain existing drainage networks will lead to devastating consequences for the communities who are affected by flooding. Figure 3.7 displays the different types of drainage networks associated with affected houses.

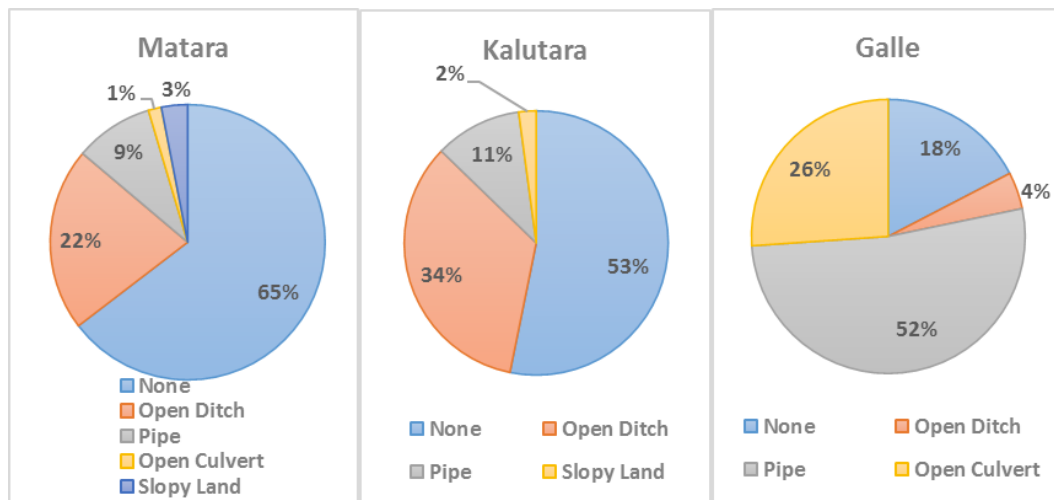


Figure 3. 7: Types of Drainage Network

The absence of proper drainage networks can be seen in more than 50 percent of houses in Matara and Kalutara districts whereas the majority of houses in Galle district, are comprised of pipes as the drainage network.

### 3.5.2 Details of surveyed flood affected houses

The details of houses were obtained during the survey, including the age of houses, materials used for the elements in building envelope and whether any technical assistance was obtained for the construction of houses.

#### 3.5.2.1 Age of Houses

The age of houses that were affected by the flood in 2017 were recorded and presented in Figure 3.8. Pursuant to the aforementioned Figure 3.8, most of the houses in all the



districts were recently built with an age of fewer than 20 years. In Matara district, a comparable number of houses were erected 20 to 40 years ago.

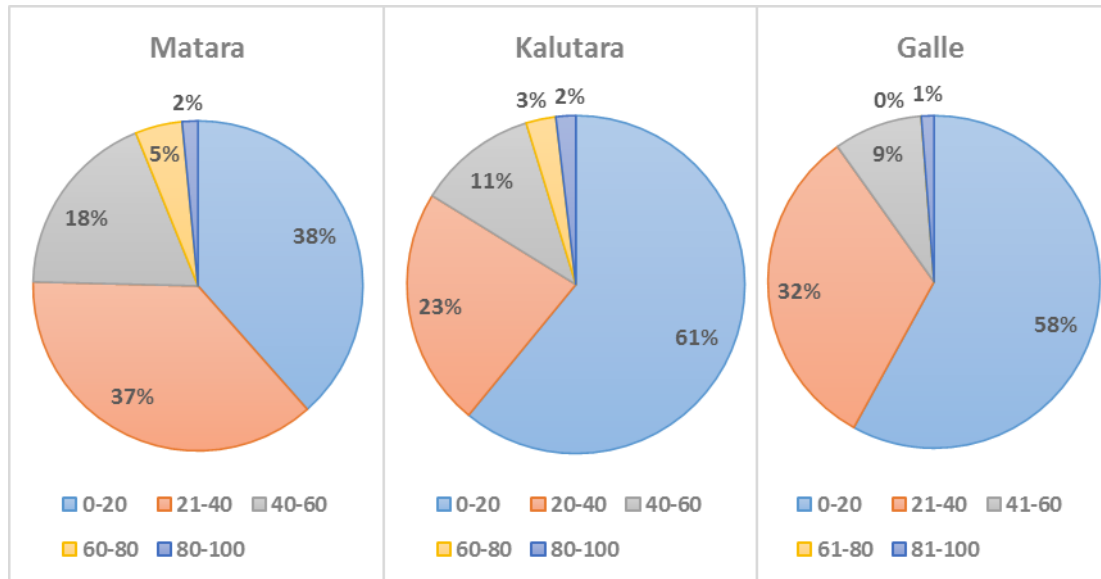


Figure 3. 8: Age of houses (Years)

### 3.5.2.2 Raw materials used for foundation

It is paramount importance that a house endangered to floods to be made out of materials which are resistant to flood damages. Different types of raw materials used for foundation construction were identified and presented in Figure 3.9. Random rubble masonry is the commonly utilized raw material for foundations in dwellings which were affected by floods.

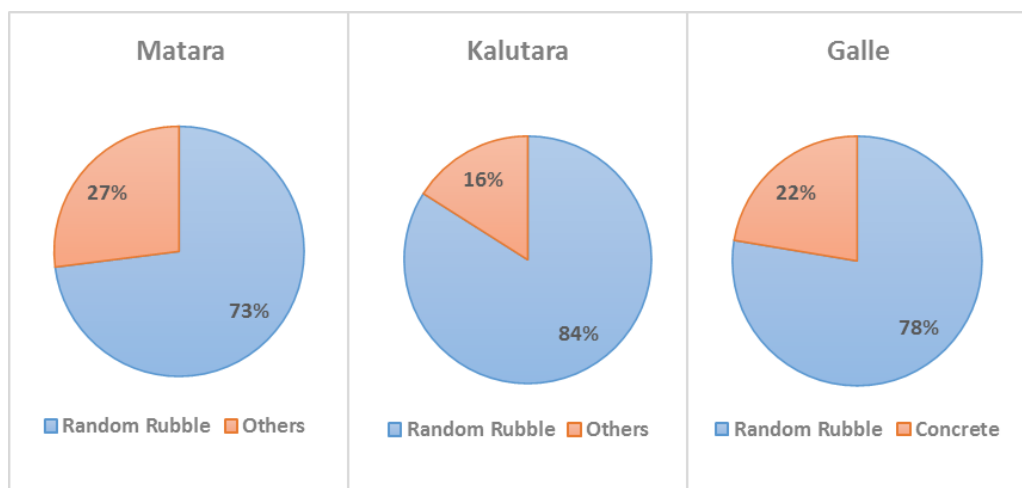


Figure 3. 9: Raw materials used for foundation

Interestingly partially weathered crushed rock was used as a foundation material exclusively in Matara district. Furthermore, except Random rubble and concrete, no other alternative materials were used in adobes located in Galle.

### 3.5.2.3 Materials used for Floors

Materials used in floor construction which were noted during the survey are presented in Figure 3.10.

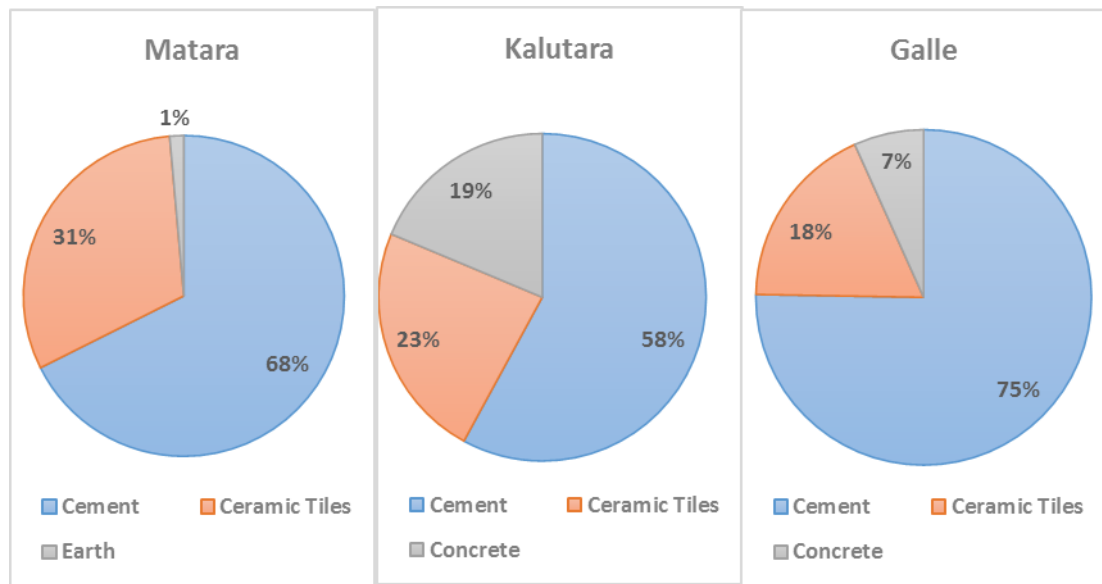


Figure 3. 10: Materials used for floors

In compliance with Figure 3.10, it can be noted that most of the floors of the flood affected houses were cement rendered. Low cost and availability of materials would have been the reason behind the selection of cement as a flooring material. However, there were few houses exclusively in Matara where compacted earth was used as the flooring material.

### 3.5.2.4. Walling Materials

A wall can be identified as one of the main victims in building envelope due to forces exerted from floods.

The selection of a suitable walling material to withstand the impacts applied on the walls from hydrostatic, hydrodynamic and impact forces is of paramount importance. Figure 3.11 elaborates on the materials used for walls in flood affected houses.

Although CB can be found as the mostly applied walling material in Kalutara and Galle district, FCB has been used by the majority of occupants in Matara. It is further noticeable that laterite blocks (*Cabook*) and Wood were distinctively used by the house owners in Matara and Kalutara respectively.

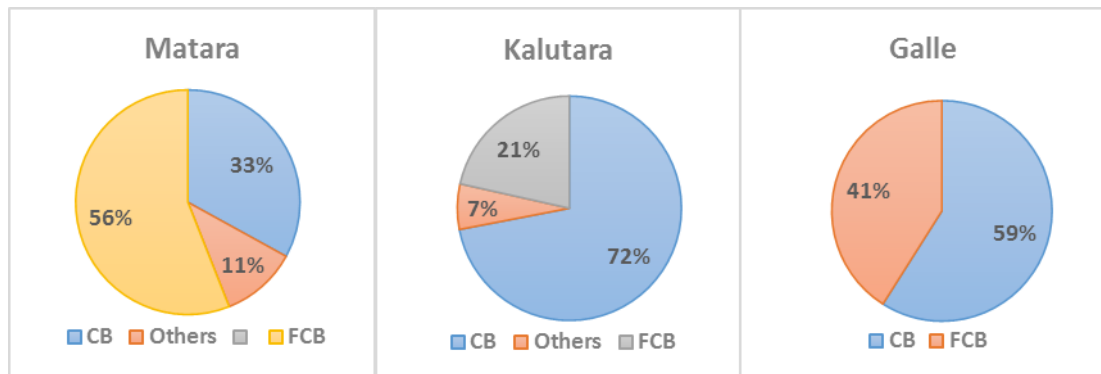


Figure 3. 11: Materials used for Walls

### 3.5.2.5 Roofing Material

Figure 3.12 highlights the materials used in the roof construction of the flood affected houses.

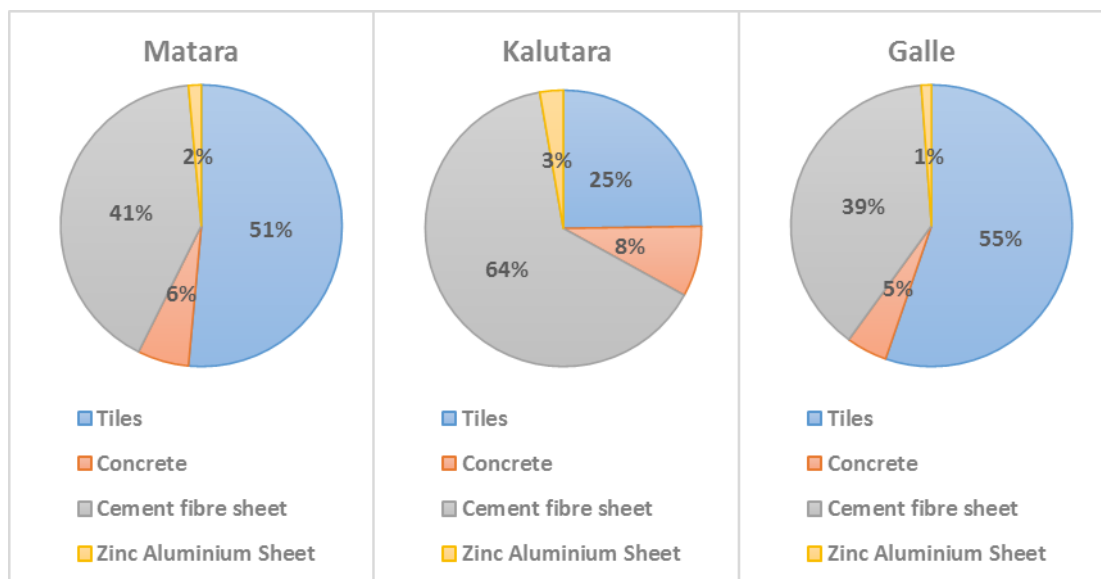


Figure 3. 12: Roofing Materials

Cement fiber sheets and tiles were used by more than 80 percent of houses in all three districts. Furthermore, the Zinc aluminum sheet was used by some of house owners.

### 3.5.2.6 Technical assistance obtained to build the houses

This aspect of the questionnaire survey was focused on obtaining any engineering or architectural assistance for the construction of dwellings. Figure 3.13 implies whether they have obtained any professional assistance.

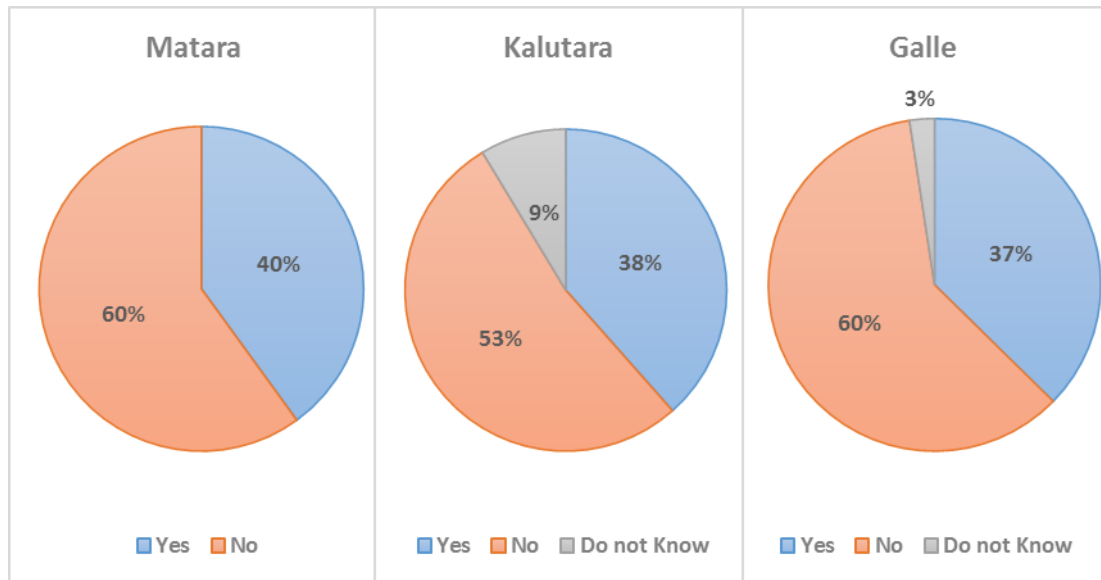


Figure 3. 13: Whether they have obtained any technical assistance

More than 50 percent of the house owners have not corresponded to any technical assistance when they were building their own homes. Furthermore, most of the house owners have initially taken guidance on architectural assistance though advice on engineering aspects was not obtained.

All the occupants of houses who have responded with the option of ‘do not know’ are the ones living on lease or rent basis in the selected houses.

### 3.5.3 Certificate of Compliance (CoC)

To maintain the quality and the standards of all constructions in Sri Lanka, the CoC has to be obtained from the relevant authorities. Figure 3.14 presents whether a CoC has been obtained from the relevant authorities or not. Here the assessors were concerned whether the occupants of the flood affected houses have got a CoC either from the Local Government Authority, National Building Research Organization or Land Reclamation Board. None of the occupants in Galle have obtained CoC from any

of the aforementioned authorities. However, in Matara and Kalutara around 20 percent of house owners have got the approval and most of those are from a local government authority.

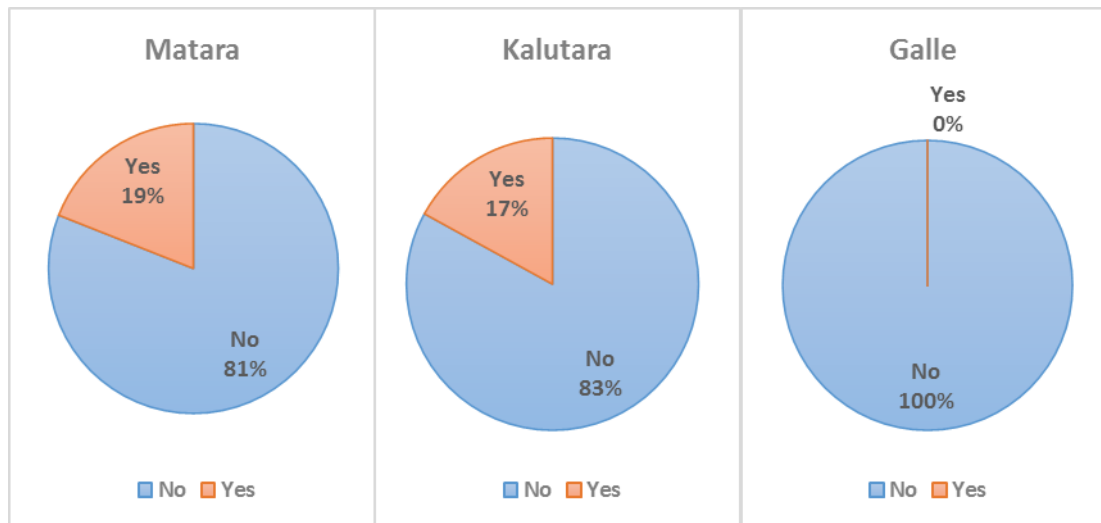


Figure 3. 14: Whether they have obtained a CoC

### 3.5.4 Physical observations due to flood

Flood height and duration were the parameters obtained under the attribute of physical observations.

#### 3.5.4.1 Flood height

Flood height would be a critical factor since the damage to a house would vary with it. The damages can be occurred due to an increase in the magnitude of forces with the rising water level. The heights of the flood and the percentage of houses affected by those flood heights are expressed in Figure 3.15.

As stated in Figure 3.15, most of the houses in Galle were facing a flood height of more than 10 feet. More than 60 percent of dwellings in Kalutara district was encountered with a flood height of fewer than four feet. However, in Matara and Galle districts higher number of houses have confronted with flood heights which are comparatively higher than houses in Kalutara.

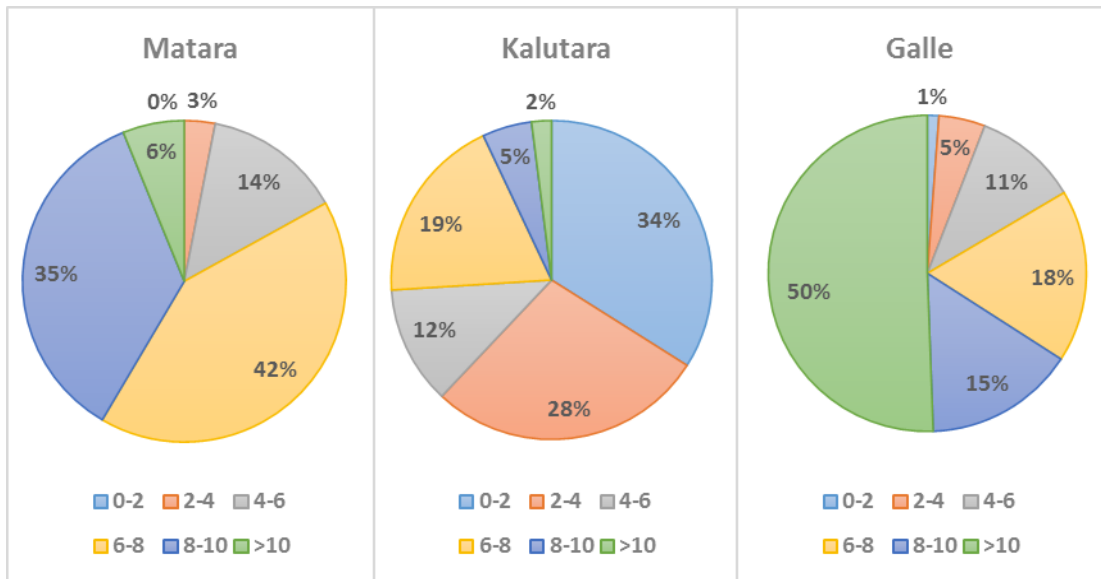


Figure 3. 15: Flood Heights (ft)

### 3.5.4.2 Inundation period

Flood duration was also recorded with the intention of assessing the inundation period. Based on this period another study was done on assessing the flexural strength of masonry walls under saturated condition. Figure 3.16 expresses the inundation period recorded (in days) in each district.

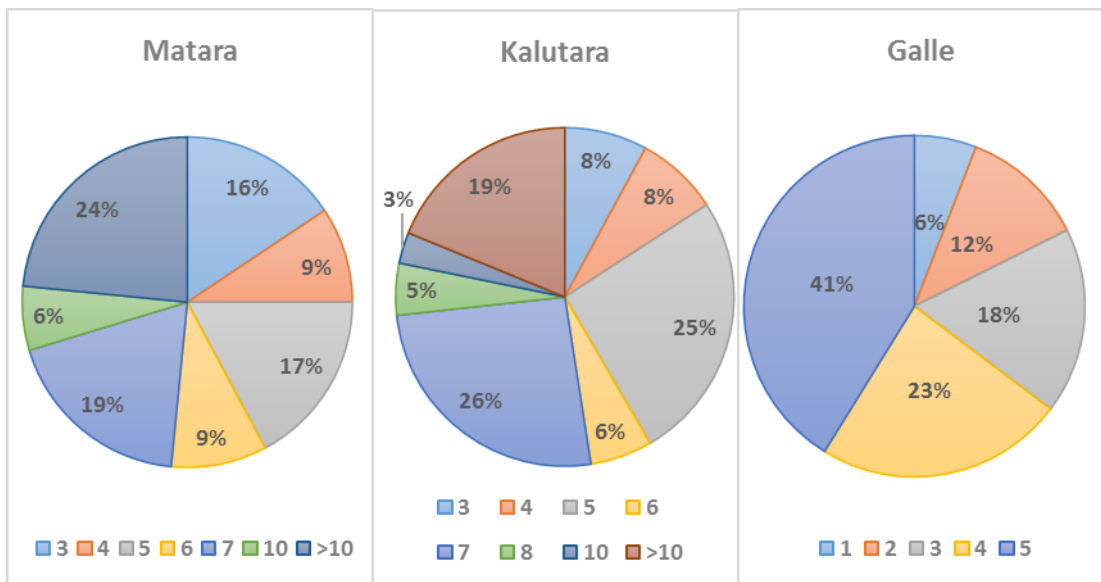


Figure 3. 16: Flood Duration (number of days)

It is quite evident that more than 50 percent of houses in Matara and Kalutara have experienced a flood duration of less than a week. However, in Galle, the maximum duration of flood water was recorded as five days. It is noticeable that around one quarter of the houses in Kalutara and Matara were flooded for more than 10 days.

### 3.5.5 Physical Impacts

The physical impacts of floods were studied in order to identify the damages that occurred to the elements of the building envelope. Figure 3.17 highlights the percentage of houses in each damaged component of the building envelope.

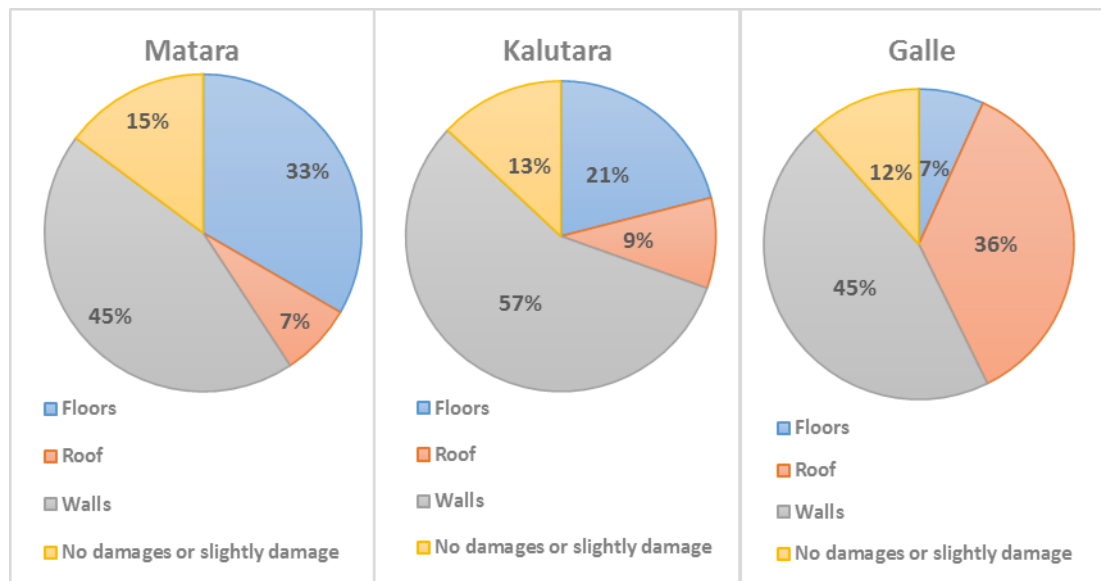


Figure 3. 17: Damages occurred to the components in building envelope

According to the aforementioned Figure 3.17, for around 50 percent of houses in Matara and Galle districts, the wall has been identified as the predominant component which was damaged in most of the houses suffered from floods. The walls were cracked or even collapsed due to possible causes such as water forces, debris impact or foundation movement. A notable observation was that most of the walls were cracked parallel to its bed joint. Figures 3.18 and 3.19 illustrate the failures that occurred on walls.

However, it is clear that the roof was damaged in majority of the houses in Kalutara. A critical observation was found to be that roof tiles have been dislodged by the floodwaters. Figure 3.21 expresses the damages emerged on the roof. The floor has

also been damaged due to the collapsing of the walls and the roof onto the floor. Damages to the floor can be visible in Figure 3.22. As demonstrated by Figure 3.23 plasterboard ceilings were also damaged by water, weakening the lining and increasing its weight and by pressure from trapped air below the ceiling.



*Figure 3. 18: Wall failed in flexure parallel to bed joint*



*Figure 3. 19: A collapsed and cracked wall*





*Figure 3. 20: Damages took place in the roof*



*Figure 3. 21: Damages occurred to the plaster board ceilings*



*Figure 3. 22: Damages emerged to the floor*

### **3.5.6 Socioeconomic Impacts**

The socioeconomic impacts of flooding can be noticed shortly after floods occur, as it immediately disrupts the daily routine of the flood affected community. Negative impacts have been created on socioeconomic life for days, weeks and even months in some areas due to this catastrophe. Roads and houses were inundated and victims were trapped due to obstruction on access roads.

The victims of flood used to stay in refugee camps located in temples and schools until they recover. Eventually, children were not able to go to colleges, employees were unable to go to workplaces and traders were struggling to start their businesses. In fact, this will create a massive negative impact on the economy.

The damages and destructions that took place on the infrastructures will lead to spending a massive number of rupees by the government of Sri Lanka in order to get back to the normalcy. Figure 3.23 emphasizes the percentage of households which were affected by the loss of days of work due to floods.

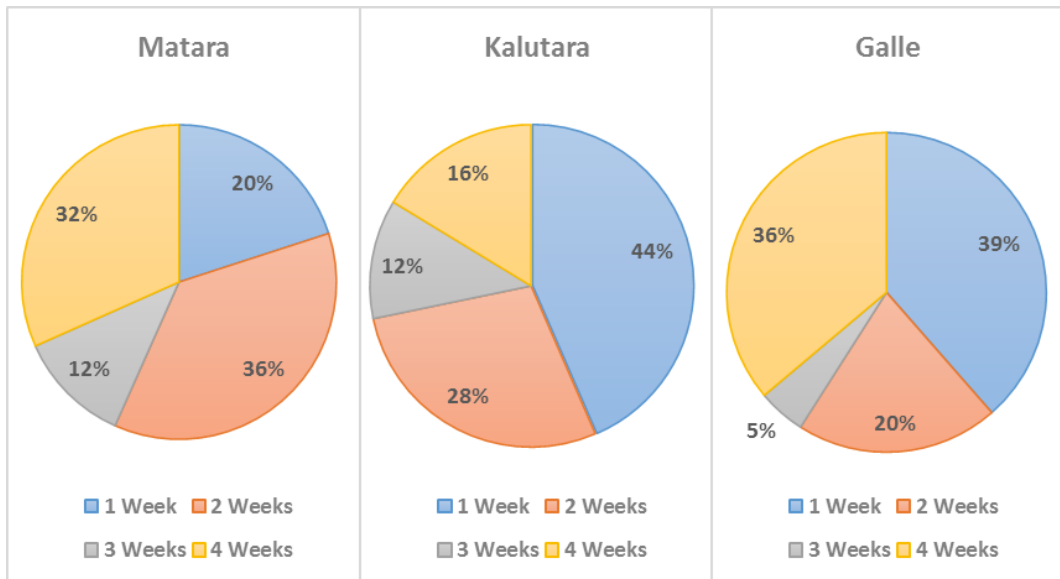


Figure 3. 23: Loss of weeks of work due to flood

As illustrated in Figure 3.23, more than 50 percent of the breadwinners in households have lost working days for nearly two weeks. However, a considerable proportion of families have lost around four weeks of working that has negatively impacted their economy.

Some details were collected based on their satisfaction with water supply, electricity and transport services. Figure 3.24 elaborates their responses on satisfaction with electricity after flooding.

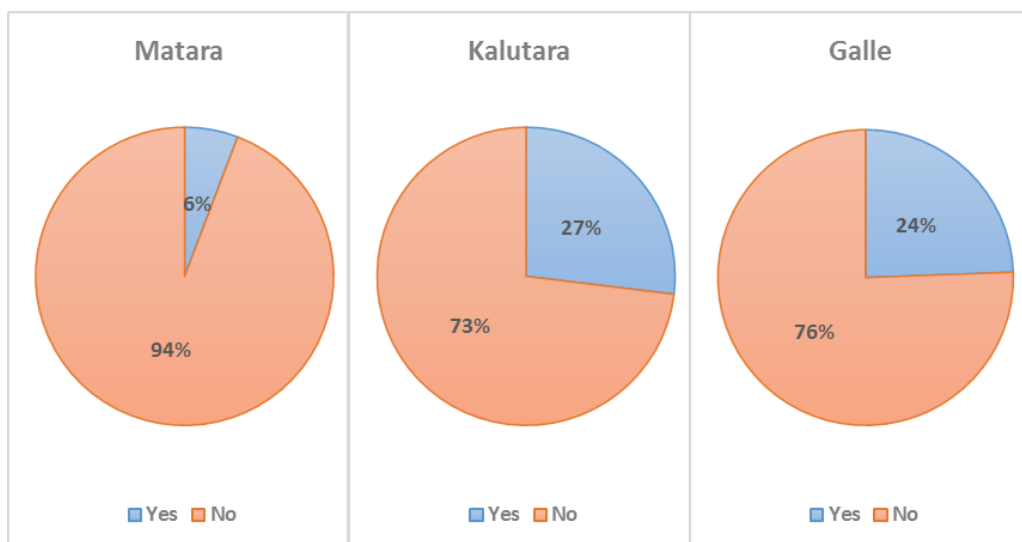


Figure 3. 24: Satisfaction with electricity

More than 70 percent of households were not satisfied with the supply of electricity after flooding; hence it is apparent that there will be a delay to restore power.

When considering water supply, most of the time the service will be restored immediately after the flood water level has fallen to an appreciable level. Most of the victims tend to leave their homes in a flood event and return to their dwellings after the flood water is reduced to a manageable level.

It is somewhat strenuous to retrieve into the regular daily routine as necessary utilities such as water and electricity have not been provided to their households. Furthermore, their houses were partially or fully damaged (Walls and Roof) and not up to standard living conditions.

The interviewers were aware of the fact that these people hesitate to move to another safe place with compensation. They were reluctant to leave their long-established houses, though it is located in a flood prone region.

It is quite apparent that an appropriate solution is required to strengthen the existing dwellings to increase the flood resistive capacity and hence to increase the flood resilience for any possible future events.

### **3.6 Proposed solution for flood resilience**

The wall has been identified as the predominant building element which is vulnerable to flood induced damages. Retrofitting of masonry walls was recommended by this research project as a measure of increasing the flood resistance.

A separate detailed study on different retrofitting techniques was conducted and elaborated later. The outcome of the research study was implemented in a demonstration house located at Bulathsinghala situated in Kalutara district.

## **4. EXPERIMENTAL STUDY**

### **4.1 Introduction**

A detailed experimental program was conducted on commonly used masonry materials (FCB and CB) for its performance under flood situations. Two different types of retrofitting materials were used (Geogrid and Wire mesh) and the wall panels were tested under the saturated condition to simulate the flood situation and were compared with that of dry situation. The aforementioned materials were selected for the complete experimental program after a detailed literature review and considering the market base available in Sri Lanka.

### **4.2 Materials used for the study**

The following section describes the materials which were used to build and retrofit masonry wall specimens.

#### **4.2.1 Masonry Units**

FCB and CB that are regularly used as walling materials in low-income houses were used for the entire experimental program. In order to reflect the practical scenario in Sri Lanka, both these unit types were purchased from a local manufacturer. The solid FCBs were acquired with nominal dimensions of 190 mm (length) x 90 mm (width) x 50 mm (height). The solid CBs were frogged on one bed face and both vertical edges with dimensions of 338 mm (length) x 94 mm (width) x 172 mm (height). The FCB and CB used are shown in Figure 4.1.



*Figure 4. 1: Masonry Units*

The locally manufactured FCB and CB were tested to determine density, porosity, initial moisture absorption, total water absorption, unit compressive and flexural strength (under dry and saturated conditions).

Randomly chosen samples of the FCB and CB were oven dried at 105°C until a fixed weight was attained. After drying, the bulk density of the units was measured prior to any of the following tests.

- I. Evaluation of compressive strength of the masonry units.
- II. Evaluation of the initial rate of water absorption of the masonry units.
- III. Evaluation of water absorption of the masonry units.

#### **4.2.1.1 Determination of the unit compressive strength of FCB and CB**

The compressive strength of the masonry units was determined as per the directions given by BE EN 1052-2 and BS EN 772-1. The method of testing is elaborated as follows.

Six specimens, each from FCB and CB that complies with the aforementioned standards were tested for both saturated and oven dry conditions. Oven dry condition was maintained using an oven at a temperature of 150°C ± 5°C until the mass was persistent and allowed to cool to ambient temperature before testing. Saturated condition of the specimens was ensured by submerging in water for 24 hours and subsequently enabled them to drain for 15 minutes.

All the specimens were tested in the orientation of the stretcher bond since that pattern was used to cast the wall panels. Figure 4.2 represents a FCB unit testing for compression. The specimen was placed in the testing machine and the load was applied at a rate of 0.05 N/mm<sup>2</sup>/s since the expected compressive strength is less than 10 N/mm<sup>2</sup>.

The maximum crushing load was recorded and eventually, compressive strength was calculated according to the standard. The compressive strength values obtained from the experiment were converted to an equivalent compressive strength relevant to an air-dry condition in order to obtain the normalized compressive strength ( $f_b$ ). Therefore, the strength values with respect to oven dried and saturated conditions were

multiplied by 0.8 (equivalent factor) and those values were multiplied once more by a shape factor (d) which was taken from the Annex A of BS EN 772-1 to obtain the normalized compressive strength.

Tables 4.1, 4.2, 4.3 and 4.4 provide the experimental results for normalized compressive strength of FCB under saturated condition and dry condition, the normalized compressive strength of CB under saturated and dry condition respectively.



*Figure 4. 2:* Testing the compressive strength of masonry units

Table 4. 1: Normalized compressive strength of FCB (oven dry condition)

Specimen Number	Length of the specimen (mm)	Width of the specimen (mm)	Maximum load achieved (kN)	Compressive strength (N/mm <sup>2</sup> )	Equivalent factor	Equivalent compressive strength (N/mm <sup>2</sup> )	Shape factor (d)	Normalized compressive strength (N/mm <sup>2</sup> )
B – 1	190.0	91.00	91.60	5.30	0.8	4.24	0.78	3.32
B – 2	187.0	92.00	73.20	4.25	0.8	3.40	0.78	2.67
B – 3	188.0	93.00	68.20	3.90	0.8	3.12	0.78	2.44
B – 4	189.0	92.00	56.00	3.22	0.8	2.58	0.78	2.02
B – 5	188.0	91.00	67.80	3.96	0.8	3.17	0.78	2.48
B – 6	186.0	93.00	97.70	5.65	0.8	4.52	0.78	3.54
<b>Average Value</b>	188.0	92.0	75.75	4.38	0.8	3.50	0.78	2.74

Table 4. 2: Normalized compressive strength of the FCB (saturated condition)

Specimen Number	Length of the specimen (mm)	Width of the specimen (mm)	Maximum load achieved (kN)	Compressive strength (N/mm <sup>2</sup> )	Equivalent factor	Equivalent compressive strength (N/mm <sup>2</sup> )	Shape factor (d)	Normalized compressive strength (N/mm <sup>2</sup> )
B – 1	183.0	93.00	68.80	4.04	1.2	4.85	0.77	3.75
B – 2	185.0	93.00	78.80	4.58	1.2	5.50	0.77	4.25
B – 3	186.0	95.00	66.40	3.76	1.2	4.51	0.77	3.49
B – 4	182.0	94.00	77.50	4.53	1.2	5.44	0.77	4.20
B – 5	188.0	92.00	79.80	4.61	1.2	5.54	0.77	4.28
B – 5	187.0	91.00	56.20	3.30	1.2	3.96	0.77	3.06
<b>Average Value</b>	185.17	93.00	71.25	4.14	1.2	4.97	0.77	3.84



Table 4. 3: Normalized compressive strength of the CB (oven dry condition)

Specimen Number	Length of the specimen (mm)	Width of the specimen (mm)	Maximum load achieved (kN)	Compressive strength (N/mm <sup>2</sup> )	Equivalent factor	Equivalent compressive strength (N/mm <sup>2</sup> )	Shape factor (d)	Normalized compressive strength (N/mm <sup>2</sup> )
C – 1	335.00	90.00	56.89	1.89	0.8	1.51	1.26	1.91
C – 2	336.00	91.00	87.49	2.86	0.8	2.29	1.26	2.90
C – 3	336.00	91.00	71.41	2.34	0.8	1.87	1.26	2.36
C – 4	336.00	90.00	44.73	1.48	0.8	1.18	1.26	1.50
C – 5	338.00	92.00	143.22	4.61	0.8	3.68	1.26	4.66
C – 6	336.00	91.00	84.35	2.76	0.8	2.21	1.26	2.79
<b>Average Value</b>	336.17	90.83	81.35	2.26	0.8	1.81	1.26	2.69

Table 4. 4: Normalized compressive strength of the CB (saturated condition)

Specimen Number	Length of the specimen (mm)	Width of the specimen (mm)	Maximum load achieved (kN)	Compressive strength (N/mm <sup>2</sup> )	Equivalent factor	Equivalent compressive strength (N/mm <sup>2</sup> )	Shape factor (d)	Normalized compressive strength (N/mm <sup>2</sup> )
C – 1	339.0	92.00	62.21	1.99	1.2	2.39	1.26	3.03
C – 2	339.0	95.00	54.95	1.71	1.2	2.05	1.26	2.59
C – 3	337.0	95.00	37.49	1.17	1.2	1.41	1.26	1.78
C – 4	340.0	94.00	60.15	1.88	1.2	2.26	1.26	2.86
C – 5	337.0	94.00	44.16	1.39	1.2	1.67	1.26	2.12
C – 6	336.0	92.00	35.13	1.14	1.2	1.36	1.26	1.73
<b>Average Value</b>	338.0	93.67	49.01	1.55	1.2	1.86	1.26	2.35

#### 4.2.1.2 Evaluation of the initial rate of water absorption of masonry units

Initial rate of water absorption of the masonry units (FCB and CB) was measured according to BS EN 772 – 11. The testing procedure is summarized as follows.

Six specimens of each type of masonry were oven dried for a temperature of  $150^{\circ}\text{C} \pm 5^{\circ}\text{C}$  until the mass was constant and allowed to cool to room temperature before they were weighed ( $m_{dry,s}$ ). The gross area of each specimen ( $A_s$ ) was determined and those were immersed in a water tray to a depth of  $5\text{mm} \pm 1\text{mm}$  with the aid of a supporting device.

Immersion time ( $t$ ) was 1 minute and the water level was maintained constant throughout the test. Specimens were removed after 1 minute and the mass of each specimen ( $m_{so,s}$ ) was measured after wiped off the surface water.

The initial rate of water absorption ( $C_{w,i}$ ) of the masonry units was calculated by using Equation 2.

$$C_{w,i} = \frac{m_{so,s} - m_{dry,s}}{A_s \times t} \times 1000 \quad (t = 1 \text{ minute}) \quad \text{Equation 2}$$

Tables 4.5 and 4.6 depict the initial rate of water absorption for FCB and CB units respectively and Figure 4.3 presents the aforementioned test carried out for FCB units.

#### 4.2.1.3 Evaluation of the water absorption of masonry units

Water absorption of the masonry units (FCB and CB) was measured according to BS EN 772 – 21. The testing procedure is briefly described below.

Six specimens were oven dried at a temperature of  $150^{\circ}\text{C} \pm 5^{\circ}\text{C}$  till the constant mass was reached and left until it comes to the ambient temperature. Mass of each specimen was measured ( $M_d$ ) and those specimens were submerged in water for  $24\text{h} \pm 0.5\text{h}$  and the mass of each specimen was measured after removing the water of the surface using a damp cloth ( $M_s$ ).

Total water absorption ( $W_s$ ) was calculated by using Equation 3.

$$W_s = \frac{M_s - M_d}{M_d} \times 100\% \quad \text{Equation 3}$$

Experimental results are presented in Table 4.7 and 4.8 for FCB and CB units respectively.

Table 4. 5: Initial rate of water absorption for FCB units

Specimen	Length (mm)	Width (mm)	Gross Area (mm <sup>2</sup> )	M <sub>dry, s</sub> (g)	M <sub>so, s</sub> (g)	C <sub>w, i</sub>
B – 1	190.00	91.00	17290.00	740	759	4.22
B – 2	187.00	92.00	17204.00	770	782	2.42
B – 3	188.00	93.00	17484.00	756	769	2.63
B – 4	189.00	92.00	17388.00	717	755	7.88
B – 5	188.00	91.00	17108.00	741	765	5.03
B – 6	186.00	93.00	17298.00	680	709	6.10
Average	188.00	92.00	17295.33	734	756	4.71



Figure 4. 3: Determination of initial rate of water absorption for FCB units

Table 4. 6: Initial rate of water absorption for CB units

<b>Specimen</b>	<b>Length (mm)</b>	<b>Width (mm)</b>	<b>Gross Area (mm<sup>2</sup>)</b>	<b>M<sub>dry, s</sub> (g)</b>	<b>M<sub>so, s</sub> (g)</b>	<b>C<sub>w, i</sub></b>
C – 1	335.00	90.00	30150.00	458	472	3.89
C – 2	336.00	91.00	30576.00	403	419	4.74
C – 3	336.00	91.00	30576.00	554	567	3.32
C – 4	336.00	90.00	30240.00	516	535	5.20
C – 5	338.00	92.00	31096.00	454	469	4.36
C – 6	336.00	91.00	30576.00	409	424	4.33
Average	336.17	90.83	30535.67	466	481	4.31

Table 4. 7: Total water absorption for FCB units

<b>Specimen</b>	<b>M<sub>a</sub> (g)</b>	<b>M<sub>s</sub> (g)</b>	<b>W<sub>s</sub> (%)</b>
B – 1	739.60	884.60	19.61
B – 2	770.10	884.60	17.61
B – 3	756.00	884.60	18.68
B – 4	717.30	884.60	18.19
B – 5	740.80	884.60	21.03
B – 6	680.00	823.70	21.13
<b>Average Value</b>	733.97	875.93	19.37

Table 4. 8: Total water absorption for CB units

<b>Specimen</b>	<b>M<sub>d</sub> (g)</b>	<b>M<sub>s</sub> (g)</b>	<b>W<sub>s</sub> (%)</b>
C – 1	457.60	494.30	8.02
C – 2	403.10	432.70	7.34
C – 3	553.90	598.40	8.03
C – 4	516.00	561.70	8.86
C – 5	453.70	495.40	9.19
C – 6	409.00	444.10	8.34
<b>Average Value</b>	465.55	504.43	8.34

A summary of the physical properties of FCB and CB units which were utilized throughout the experiment is detailed in Table 4.9.

Table 4. 9: Summary of the properties of masonry units

<b>Type</b>	<b>FCB</b>		<b>CB</b>	
<b>Avg. Dimensions (Length × Width × Thickness)</b>	188mm x 92mm x 50mm		335mm x 170mm x 90mm	
<b>Condition</b>	Saturated	Oven Dry	Saturated	Oven Dry
<b>Compressive Strength (N/mm<sup>2</sup>)</b>	4.14	4.38	1.55	2.65
<b>Water absorption coefficient</b>	19.37%		8.34%	
<b>Initial rate of water absorption coefficient</b>	4.71		4.31	

#### **4.2.2 Mortar**

The mortar used to cast and render the wall panels were tested for physical properties according to standards BS EN 1015-3, 1015-11 and 1015-18 which comprise the determination of consistence of fresh mortar by flow table, determination of flexural and compressive strength of hardened mortar and ascertain water absorption coefficient due to the capillary action of hardened mortar respectively.

Three number of mortar cubes (each with dimensions of 40 mm x 40 mm x 160 mm) were prepared from each series of constructed wall panels and plaster applications. These were first tested in flexure, with two broken sections used to determine the compressive strength and water absorption coefficient.

Masonry wall panels were erected using 1:6 cement: sand mortar with the plaster having a 1:5 ratio. Ordinary portland cement and river sand containing fine aggregates were the main constituents in the mortar which represent materials extensively used in Sri Lankan masonry construction. In order to simulate the local conditions, the mortar was mixed manually by experienced masons with water content controlled by workability.

##### **4.2.2.1 Determination of consistence of fresh mortar (by flow table)**

The flow values were determined using the flow table in the fresh mortar which was obtained from the mason's board as representative samples of each mortar batch. This test depicts fluidity or wetness of the fresh mortar and gives an indication of deformability in fresh mortar when subjected to a certain type of stresses.

Flow table, truncated conical mold, tamper and other necessary apparatus were arranged as per the standard. Two fresh mortar samples were taken from each batch of mortar to measure the average flow values. The disc of the flow table, inner surface and perimeters of mold were rubbed and cleaned with a wet cloth and let those dry before each test.

The mold was placed in the center of the disc after applying oil on disc and inner surface. It was filled by two mortar layers and tamped those aforementioned layers for 15 short strokes to make sure uniform filling of mortar. Figure 4.4 illustrates the mold

filled with mortar after compaction. Excess mortar and water were removed and cautiously cleaned the free area of the disc. After 15 seconds the mold was raised vertically and Figure 4.5 demonstrates the mortar after removing the mold. The flow table was jolted 15 times at a constant frequency of approximately one per second to spread out the mortar on the disc. Figure 4.6 shows the expanded mortar after jolting. Finally, the diameters of the mortar in two directions at right angles were obtained in order to find the consistency of fresh mortar. Table 4.10 and 4.11 present the flow values of mortar used to cast and render with different types for FCB and CB wall panels respectively.



*Figure 4. 4: Compacted mortar in the mold*



*Figure 4. 5: Condition of the mortar after removing the mold*

All the average diameters were deviated from their initial individual diameters by less than 10%. Hence the flow value of each batch of mortar can be considered as an average diameter of the spread mortar in each respective batch.



*Figure 4. 6: Mortar after jolting for 15 seconds*

#### **4.2.2.2 Determination of mean compressive strength, flexural strength and water absorption coefficient of hardened mortar**

Mean compressive strength and flexural strength of the mortar used to cast and render wall panels were determined in accordance with BS EN 1015-11. A three-point loading testing method was carried out until failure in order to ascertain the flexural strength of mortar.

The compressive strength of mortar was determined using a fragment (half piece) which was broken during the flexural testing. The metal mold, tamper and other apparatus were arranged as per the aforementioned standard. Three mortar specimens were cast from each batch of mortar by using the metal mold and the size of each specimen was 160 mm × 40 mm × 40 mm.

Before casting prisms, the mold frame was connected and clamped together at right angles and internal faces of the mold were cleaned and lubricated to prevent adhesion of the mortar. The mold was filled with mortar in two nearly equal layers and each layer was compacted with 25 strokes using the tamper. The excess mortar was removed and the top surface was leveled using a trowel. Specimens were removed from the



mold cautiously after 24 hours and they were kept and cured in accordance with the conditions stated in BS EN 1015-11.

Table 4. 10: Flow values of mortar used to cast and render with different conditions for FCB wall panels

Types of Wall Panels	Mortar used for Casting		Maximum deviation from the average diameter (%)	Mortar used for Rendering		Maximum deviation from the average diameter (%)
	Dia. 01 (mm)	Dia. 02 (mm)		Dia. 01 (mm)	Dia. 02 (mm)	
<b>Without retrofitting and rendering (Saturated)</b>	130	128	0.78	-	-	-
<b>Without retrofitting and rendering (Dry)</b>	120	125	2.04	-	-	1.96
<b>Rendering only (Saturated)</b>	120	115	2.13	120	115	2.13
<b>Rendering only (Dry)</b>	125	130	1.96	110	115	2.22
<b>Wire mesh (Saturated)</b>	120	115	2.13	120	115	2.13
<b>Wire mesh (Dry)</b>	110	115	2.22	125	130	1.96
<b>Geogrid (Saturated)</b>	120	115	2.13	125	128	1.19
<b>Geogrid (Dry)</b>	125	130	1.96	126	127	0.40

Table 4. 11: Flow values of mortar used to cast and render with different conditions for CB wall panels

	Mortar used for Casting		Maximum deviation of the average diameter (%)	Mortar used for Rendering		Maximum deviation of the average diameter (%)
	Dia. 01 (mm)	Dia. 02 (mm)		Dia. 01 (mm)	Dia. 02 (mm)	
<b>Without retrofitting and rendering (Saturated)</b>	125	130	1.96	-	-	-
<b>Without retrofitting and rendering (Dry)</b>	124	127	1.20	-	-	-
<b>Rendering only (Saturated)</b>	125	122	1.21	125	128	1.19
<b>Rendering only (Dry)</b>	126	119	2.86	126	127	0.40
<b>Wire mesh (Saturated)</b>	128	124	1.59	125	130	1.96
<b>Wire mesh (Dry)</b>	127	120	2.83	124	127	1.20
<b>Geogrid (Saturated)</b>	129	125	1.57	125	122	1.21
<b>Geogrid (Dry)</b>	124	123	0.40	126	119	2.86

Specimens were tested for flexure immediately after testing the respective wall panels for flexure. The load was applied without a shock at a uniform rate in the range between 10 N/s to 50 N/s. Figure 4.7 displays a three-point loading flexural strength testing of a mortar cube. Maximum load applied until failure on the specimen was recorded and the flexural strength was calculated by using Equation 4. One half of the broken prism from the flexural testing was taken to find the compressive strength.

$$f = 1.5 \frac{Fl}{bd^2} \text{ (N/mm}^2\text{)} \quad \text{Equation 4}$$

$F$  - maximum load applied to the specimen (N)

$l$  - distance between the axis of support

$b$  and  $d$  are internal mold dimensions (breadth and depth)



*Figure 4. 7: Flexural Testing of a mortar prism*

Compressive strength was calculated by dividing the maximum failure load from the cross-sectional area of the specimen. Figure 4.8 shows the compression testing of a mortar prism.

Other half of the broken prism was taken to ascertain the water absorption coefficient due to the capillary action as per BS EN 1015-18. Specimens were dried to a constant mass in a ventilated oven at a temperature of 60 °C. Dry mass of each specimen was recorded and subsequently placed on a tray and immersed in water to a depth of 5 mm to 10 mm.

Those were removed from the tray after 10 minutes and wiped off the surface water rapidly with a dampened cloth. Eventually, the weight of the specimen was measured ( $M_1$ ) and put back them immediately into the tray. The same

procedure was repeated after 90 min and the weight of the specimen was measured ( $M_2$ ).

Figure 4.9 depicts the arrangement for the testing of water absorption in mortar prisms. The coefficient of water absorption was calculated by using Equation 5.

$$C = 0.1(M_2 - M_1) \text{ kg/m}^2 \text{ min}^{0.5} \quad \text{Equation 5}$$



*Figure 4. 8:* Compression testing of a mortar prism

Those were removed from the tray after 10 minutes and wiped off the surface water rapidly with a dampened cloth. Eventually, the weight of the specimen was measured ( $M_1$ ) and put back them immediately into the tray. The same procedure was repeated after 90 min and the weight of the specimen was measured ( $M_2$ ). Average experimental results obtained from the aforesaid experiments are presented in Table 4.12 and 4.13.



*Figure 4. 9:* Testing arrangement for water absorption coefficient of mortar prisms

Table 4. 12: Physical properties of mortar used for FCB wall panels

Retrofitting Type	Flexural Strength ( $Nmm^2$ )		Compressive Strength ( $Nmm^2$ )		Water absorption coefficient ( $kg/m^2min^{0.5}$ )	
	Mortar Cubes from Casting	Mortar Cubes from Rendering	Mortar Cubes from Casting	Mortar Cubes from Rendering	Mortar Cubes from Casting	Mortar Cubes from Rendering
Without retrofitting and rendering (Saturated)	1.71	-	5.6	-	1.15	-
Without retrofitting and rendering (Dry)	2.45	-	6.32	-	0.76	-
Rendering only (Saturated)	2.93	1.8	9.46	4.36	0.78	1.14
Rendering only (Dry)	2.02	1.98	6.01	4.56	0.93	0.98
Wire mesh (Saturated)	2.93	1.4	9.46	4.36	0.78	1.19
Wire mesh (Dry)	2.22	2.32	4.54	4.44	0.83	1.4
Geogrid (Saturated)	2.08	1.18	6.52	4.97	1.05	1.28
Geogrid (Dry)	2.08	1.18	6.52	4.97	1.05	1.28

Table 4. 13: Physical properties of mortar used for CB wall panels

Retrofitting Type	Flexural Strength ( $Nmm^2$ )		Compressive Strength ( $Nmm^2$ )		Water absorption coefficient ( $kg/m^2min^{0.5}$ )	
	Mortar Cubes from Casting	Mortar Cubes from Rendering	Mortar Cubes from Casting	Mortar Cubes from Rendering	Mortar Cubes from Casting	Mortar Cubes from Rendering
Without retrofitting and rendering (Saturated)	1.71	-	5.6	-	1.15	-
Without retrofitting and rendering (Dry)	1.98	-	6.7	-	1.26	-
Rendering only (Saturated)	1.55	1.8	5.05	4.34	0.9	1.14
Rendering only (Dry)	3.01	2.06	8.1	6.92	0.95	1.25
Wire mesh (Saturated)	1.55	1.19	5.05	5.09	0.92	1.13
Wire mesh (Dry)	2.22	2.32	9.46	4.36	0.83	1.4
Geogrid (Saturated)	2.02	1.74	7.28	5.32	0.93	1.21
Geogrid (Dry)	2.02	1.32	7.28	5.89	0.93	1.08

#### 4.2.3 Retrofitting Materials

Two reinforcing materials were selected for the study are presented here. Geogrid made out of stretched, monolithic polypropylene (PP) flat bars with

welded junctions was used as one retrofitting material in the research. The other type of retrofitting material was the polyvinyl chloride (PVC) coated wire mesh which is welded and coated with a protective layer of zinc on steel fabric and PVC fuse bonded to the wire. Figures 4.10 and 4.11 illustrate the geogrid and wire mesh which were applied in the study. Further, the material properties of the retrofitting types are indicated in Table 4.14.

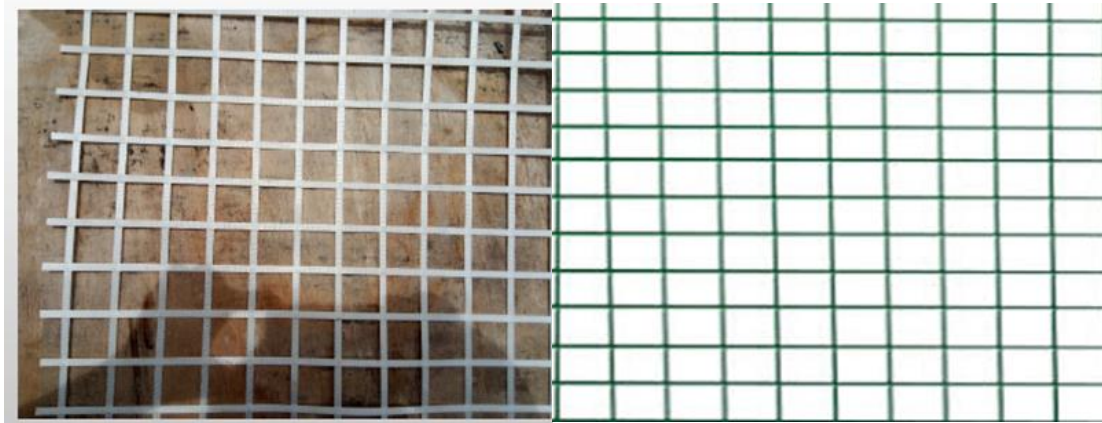


Figure 4. 10: Geogrid

Figure 4. 11: PVC coated welded wire mesh

Table 4. 14: Properties of wire mesh and geogrid

	<b>Geogrid</b>	<b>Wire Mesh</b>
<b>Raw Material</b>	Poly propylene, white color	Low carbon steel wire with PVC powder
<b>Mass per unit area (g/m<sup>2</sup>)</b>	240	320
<b>Maximum tensile strength (KN/m)</b>	23.6	17.8
<b>Aperture Size (mm×mm)</b>	33×33	25×25
<b>Cost per square meter (SLR)</b>	595.00	360.00

### 4.3 Construction of masonry wall panels

In order to test masonry walls for its flexural strength parallel to bed joint, eighty (80) number of wall panels were constructed for the experimental program. The FCB panels were 400mm wide and with a height of 470 mm and the CB wall panels were 520 mm wide and with a height of 562.5 mm were constructed with a bed joint thickness of 17.5 mm and in stretcher bond pattern. The wall panels were cured for 14 days for curing and maintained to be undisturbed before applying the retrofitting materials on one side of the panel (wire mesh and geogrid).

The variables introduced in the experimental program are all indicated in Figure 4.12. For each variable five (5) number of panels were constructed as per BS EN 1052-2. Wall panels were pre compressed to a given vertical stress of  $2.5 \times 10^{-3} Nmm^2 - 5 \times 10^{-3} Nmm^2$  according to BS EN 1052-2 immediately after constructing them. Initially, one face of the wall was rendered with a thickness around 8 mm and then the retrofitting material was embedded into that rendered layer.

The final rendered thickness was finished up to 17.5 mm. Wall panels were kept for 28 days after retrofitting and before testing for flexure. The wall panels needed to be saturated were immersed in water for 24 hours before testing for flexure. Figure 4.13 represents the steps followed during the erection of wallets in the experimental program.

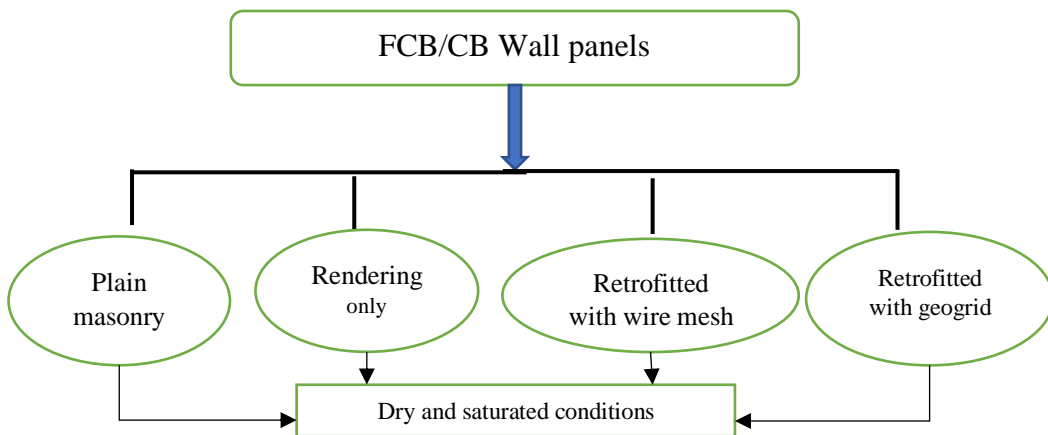


Figure 4. 12: Different variables introduced for wall panel construction





**Step 1: FCB wall panels casting**



**Step 2: CB wall panels casting**



**Step 3: Pre compression applied on FCB wall panels**



**Step 4: Pre compression applied on CB wall panels**



**Step 5: Applying the wire mesh and rendering up to 17.5 mm thickness after 14 days of curing**



**Step 6: Applying the geogrid and rendering up to 17.5 mm thickness after 14 days of curing**



**Step 7: Saturation of specimen for 24 hours after 28 days of retrofitting (applicable for saturated condition)**



**Step 8: Testing arrangement for FCB wall panels**



**Step 9: Testing arrangement for CB wall panels**



**Step 10: Recording the ultimate loads**

*Figure 4. 13: Steps followed from construction to testing of wall panels*

#### **4.4 Testing of wall panels for flexure parallel to bed joint**

All masonry panels were tested for flexure parallel to bed joint as per the standard BS EN 1052-2. The experimental setup and the apparatus that was utilized to insert the load are shown in Figure 4.14. The height difference from the outer bearings and end of the specimen was greater than 15mm. Inner bearings were maintained as 0.4 - 0.6 times height difference of outer bearings and they were placed at the center within two adjacent mortar joints.

Distance between inner bearings and outer bearings was consistently larger than the thickness of a masonry unit as expressed in the aforementioned standard. The loading rate was maintained at a rate between  $0.03 \text{ N/mm}^2/\text{min}$  and  $0.3 \text{ N/mm}^2/\text{min}$  and the highest load applied to each specimen prior to the failure was recorded in order to determine the flexural strength.

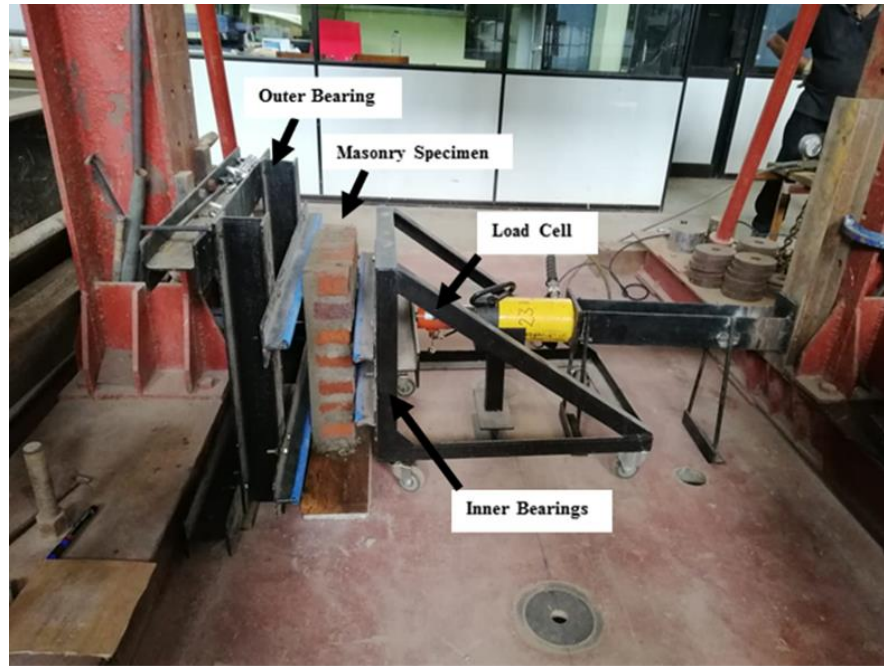


Figure 4. 14: Experimental Setup

#### 4.5 Experimental Results

The ultimate load applied on the wall panel just before the flexural failure was recorded and subsequently, the flexural strength was calculated according to the standard of BS EN 1052-2 using Equation 6.

$$f_{xi} = \frac{3F_{i,max}*(l1-l2)}{2bt_u^2}(\text{N/mm}^2) \quad \text{Equation 6}$$

Where,

$f_{xi}$  Flexural strength of masonry specimen

$F_{i,max}$  The maximum load applied to an individual masonry specimen

$l1$  Spacing of the outer bearings

$l2$  Spacing of the inner bearings

$b$  Width of the masonry specimen

$t_u$  Width of the masonry unit

Average flexural strength parallel to bed joint for each type of masonry wall panel is presented in Table 4.15 and 4.16.

Table 4. 15: Average flexural strength parallel to bed joint of FCB wall panels

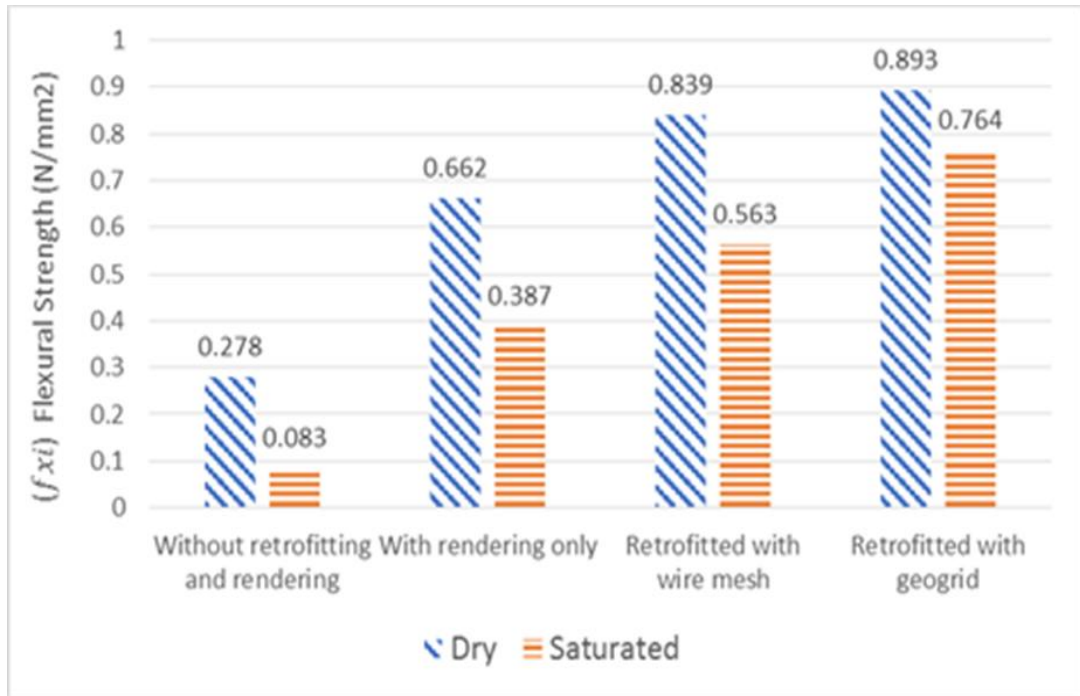
<b>Retrofitting Type</b>	<b>Condition of the specimen</b>	<b>Average Flexural Strength (N/mm<sup>2</sup>)</b>	<b>Covariance</b>
Without retrofitting and rendering	Saturated	0.083	0.303
Without retrofitting and rendering	Dry	0.278	0.247
Rendering only	Saturated	0.387	0.141
Rendering only	Dry	0.662	0.065
Wire mesh	Saturated	0.563	0.256
Wire mesh	Dry	0.839	0.078
Geogrid	Saturated	0.764	0.198
Geogrid	Dry	0.893	0.085

Table 4. 16: Average flexural strength parallel to bed joint of CB wall panels

<b>Retrofitting Type</b>	<b>Condition of the specimen</b>	<b>Average Flexural Strength (N/mm<sup>2</sup>)</b>	<b>Covariance</b>
Without retrofitting and rendering	Saturated	0.135	0.366
Without retrofitting and rendering	Dry	0.151	0.379
Rendering only	Saturated	0.55	0.206
Rendering only	Dry	0.846	0.080
Wire mesh	Saturated	0.606	0.097
Wire mesh	Dry	0.861	0.092
Geogrid	Saturated	0.784	0.295
Geogrid	Dry	0.945	0.081

#### 4.6 Analysis of experimental results

The variation of flexural strength parallel to bed joint for FCB wall panels with and without retrofitting are indicated in Figure 4.15.



*Figure 4. 15:* Variation of flexural strength parallel to bed joint for FCB wall panels. The results are displayed for both dry and saturated conditions. It is recognizable that the flexural strength in saturated condition was discovered to be less than that of the dry condition for the FCB wall panels. Maximum flexural strength was obtained for the dry FCB wall panel retrofitted with geogrid and the minimum was recorded for the saturated FCB wall panel without retrofitting and rendering.

Another observation was that the flexural strength of panels retrofitted with wire mesh in the dry condition found to be relatively similar with wall panels retrofitted with geogrid. However, there is an interesting reduction in flexural strength of wall panels retrofitted with wire mesh in a saturated condition when compared with geogrid.

The aforementioned matching circumstance can be visible for CB wall panels. The diversification of flexural strength parallel to bed joint for the CB wall panels under divergent conditions are introduced in Figure 4.16.

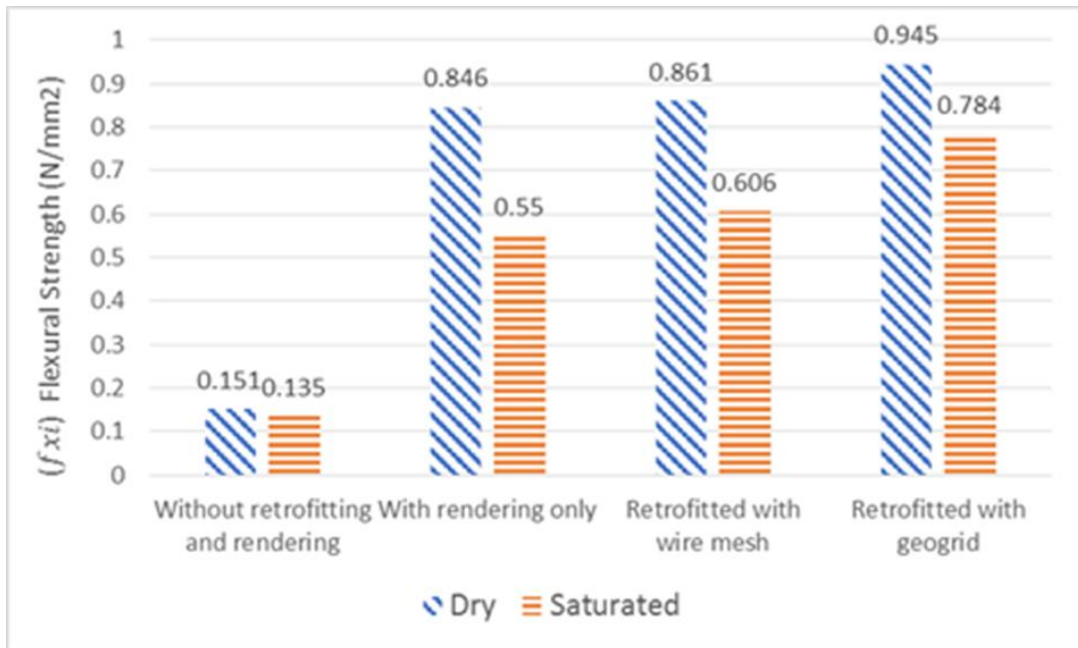


Figure 4. 16: Variation of flexural strength parallel to bed joint for CB wall panels

#### 4.6.1 Strength increase in flexural strength (parallel to bed joint) with different types of retrofitting

Figure 4.17 presents the increase in flexural strength due to different types of retrofitting under both dry and saturated condition of FCB wall panels.

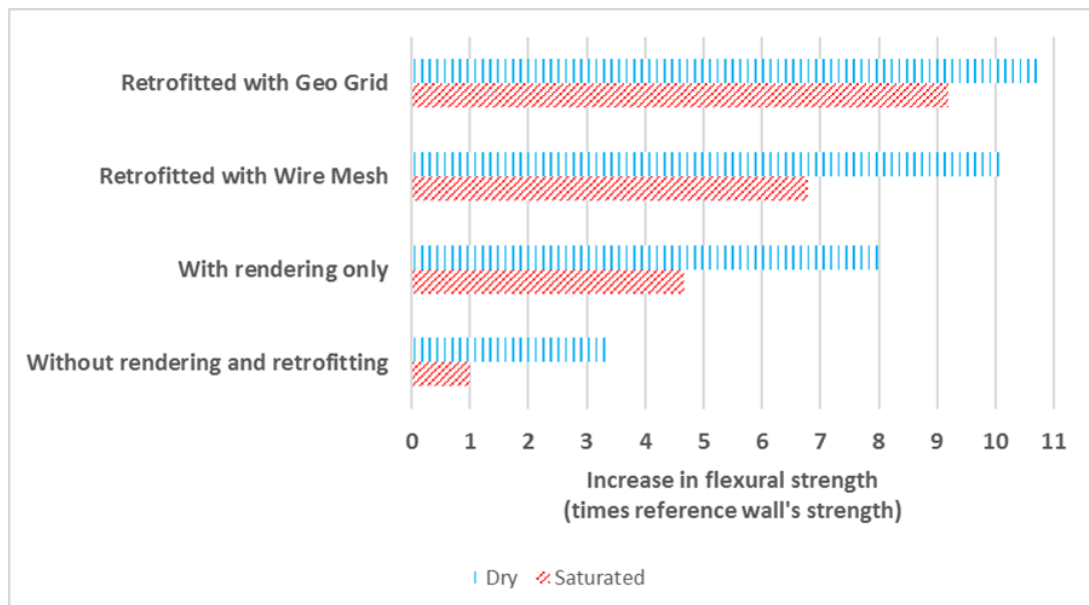
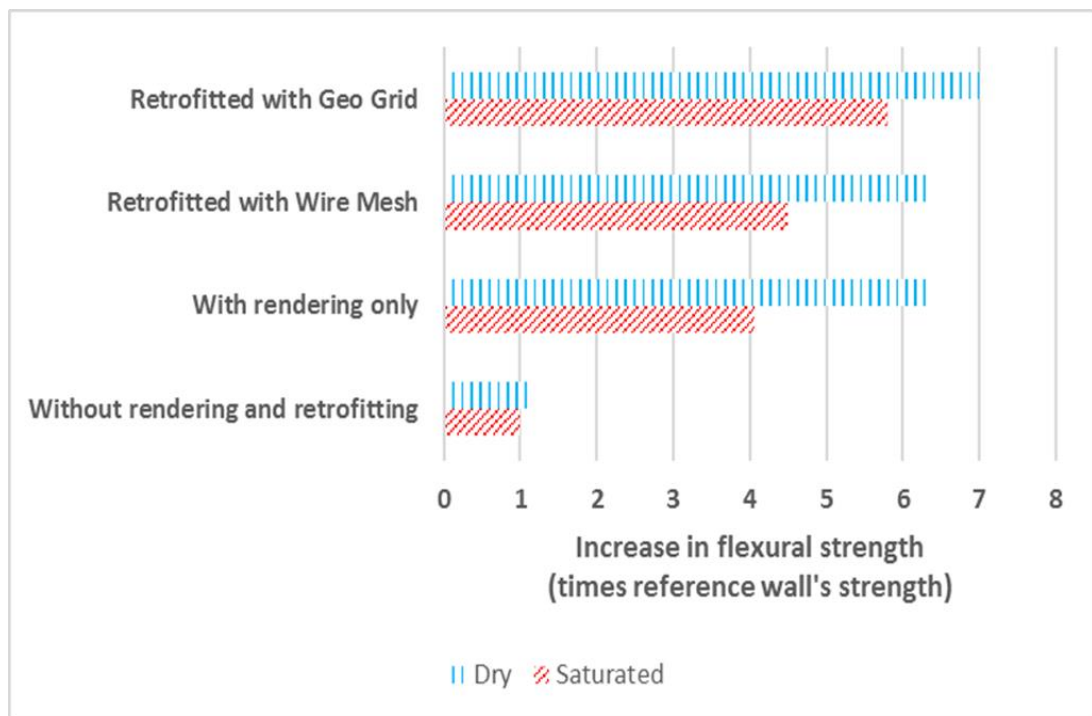


Figure 4. 17: Flexural strength increase in parallel to bed joint of retrofitted FCB wall panels

The panels retrofitted with geogrid under saturated condition have manifested 9.2 times the strength of the reference wall panel which is subjected to a saturated condition and without any retrofitting or rendering. The wall panels retrofitted with wire mesh in a saturated condition have appeared 6.78 times flexural strength of the reference panel. The FCB wall panels with rendering only in a saturated condition have reported a strength increase of 4.66 times than the reference wall. Figure 4.18 presents the strength increase due to different types of retrofitting under both dry and saturated condition of CB wall panels.



*Figure 4. 18:* Increase in flexural strength parallel to bed joint of retrofitted CB wall panels

The panels retrofitted in saturated condition retrofitted with geogrid have reported 5.8 times the strength of reference wall panels which is subjected to saturate condition and without any retrofitting or rendering. The wall panels retrofitted with wire mesh in saturated condition have illustrated 4.5 times increase in flexural strength than the reference panel. The CB wall panels with rendering alone in saturated condition have shown a strength increase of 4.07 times than the reference wall. Table 4.17 illustrates the percentage increase of flexural strength values compared with dry plain masonry.



Table 4. 17: Percentage increase of the flexural strength values compared with dry plain masonry

Type of wall panel	Condition of the specimen	CB	FCB
		% increase in flexural strength compared to the dry state of plain masonry	
Plain Masonry	Saturated	-10.6	-70
Rendering only	Dry	460	138
	Saturated	264.2	39.2
Rendering and retrofitted with wire mesh	Dry	470	201
	Saturated	301	102.5
Rendering and retrofitting with geogrid	Dry	525	221
	Saturated	419.2	174.8

#### 4.6.2 Impact of saturation of wall panels under flood situation

In order to represent the wall panels subjected to a flood situation, the flexural strength was assessed under a saturated condition. The strength reduction as a result of the saturation is elaborated in Figure 4.19 for different retrofitting types.

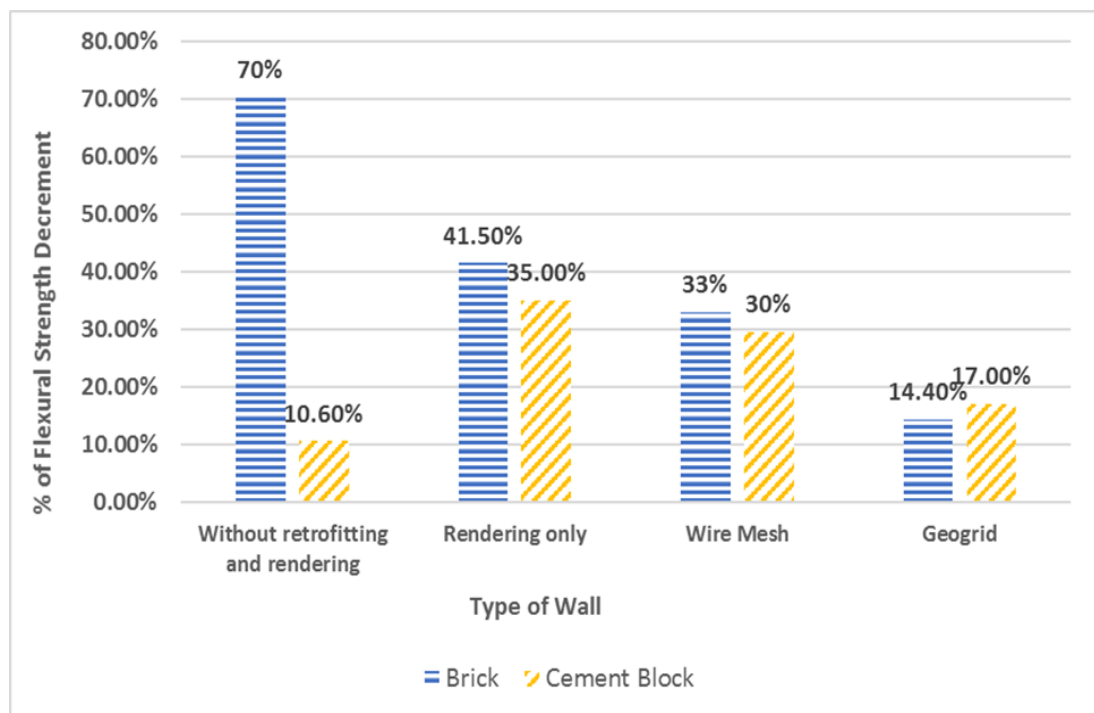


Figure 4. 19: Percentage reduction of flexural strength of masonry wall panels from dry condition to saturated condition

The FCB wall panels without any retrofitting and rendering have depicted a 70% reduction in saturation however the CB wall panels without retrofitting and rendering have reported a 10.6% reduction.

Once the walls are rendered, the strength difference for FCB walls become 41.5% whereas the CB indicates a 35% reduction. So, there is a decreasing trend of strength reduction with retrofit specifying 33% for BCB wall panels and a 30% reduction in CB wall panels with wire mesh.

The lowest reduction of strength was noted for wall panels retrofitted with geogrid showing a 14.4% for FCB wall panels and a 17% for CB wall panels. This outlines the geogrid as a retrofitting material that performed best out of two types of retrofitting in terms of flexural strength parallel to bed joint.

#### **4.6.3 Failure types observed in wall panels during the experimental program**

Distinct types of failure patterns were noticed throughout the experimental program for divergent categories of tested wall specimens and they could be listed as follows.

1. Horizontal flexural crack in the rendered face of the wall panel.
2. Diagonal crack in the rendered face of the wall panel.
3. Shear failure closer to the supports of the wall panel (Wall did not fracture into pieces).
4. Crack occurred across the interface between the wire mesh and the rendered surface and the external cement plaster was move apart from the wire mesh.
5. Wire mesh was torn at failure.
6. Bed joint failure.
7. Crack in the masonry unit of a wall panel.

The above failure patterns which were observed during the experimental program are represented in Figure 4.20.



Horizontal flexural crack



Diagonal crack



Brittle failure



Shear failure



Separation of retrofitting material and external plaster



Wire mesh was broken



Crack along the bed joint



Crack in the masonry unit

*Figure 4. 20: Observed failure patterns during the experimental program*

#### 4.6.4 Cost Study

A cost study was carried out in the experimental program by taking into account of rendering and retrofitting of thirty (30) masonry wall panels which were cast within six days. Variables such as labor hours and cost for the panels were recorded in each day and Table 4.18 presents the average values of the aforementioned variables per one square meter area of wall panel.

The wall panels constructed with rendering only were reported with the lowest cost. Although wall panels retrofitted with geogrid reported with an 19 % cost increase compared to that of wire mesh or an overall increase of 73% over that of the rendered only panels, the extra cost is outweighed by the 32.3% and 51.9% improvement in flexural strength for CB and FCB wall panels respectively throughout saturated conditions which designate a 24- hour flood. Hence geogrid performs better in terms of flexural strength out of the selected retrofitting materials.

Table 4. 18: Cost per square meter of wall panel

Wall Type	Labour hours		Cost of retrofitting Material	Total cost
	Skilled	Un Skilled	(LKR)	(LKR)
Rendering only	1.15	0.57	-	855.00
Retrofitted with wire mesh	1.72	0.86	360.00	1244.30
Retrofitted with geogrid	1.72	0.75	595.00	1480.00

## **5. Practical application of the outcome from the experimental program**

A house at Bulathsinhala in Kalutara district was selected to apply the research outcome. This house was heavily damaged due to overflow of *Kukule ganga* in 2017 floods. Therefore, it is of paramount importance to increase the disaster resistance of this house in an event of future flooding.

As many of these houses are built with FCB and CB which are produced in cottage industry have different properties of strength, water absorption etc. throughout the country. Randomly selected samples of bricks and blocks which were used for the experiment program have showed lack of compression and flexural capacity in dry condition. Hence it is inevitable that those aforementioned strength parameters would considerably decline in saturated condition.

The walls are subjected to a saturated condition when they are exposed to floods and it is important to retrofit them in order to increase resistivity of the structure to additional lateral loads induced by floods. Furthermore, it permits occupants to get back to their residents within a short period of time since there are minimal structural related renovations to be completed in those dwellings.

1m height of the wall from bottom was retrofitted since most of the windows are placed lower than 1m height from sill to finish grade when considering the potential hydraulic gradient. The geogrid was pinned from the bottom of the wall to the ground in order to ensure a proper fixity.

The chosen four-bedroom 1532 sq. ft. house was built in year 2000 for a family of 6 members after being resettled in 1995 due to landslide threat in Heenpadura (Bulathsinghala). The walls of the house are rendered and of mixed construction with exterior walls made of FCB and inner walls of CB. The structure is built upon a rubble foundation with no columns and the single unit gable roof is sheeted with corrugated asbestos.

The structure was exposed to flood water depths of 4, 4, 9, and 16 feet (1.22, 1.22, 2.74, and 4.88 m) in 2003, 2007, 2013 and 2017 respectively. The occupants reported no observed flooding prior to the construction of *Kukuleganga* reservoir apart from the annual flooding of the nearby paddy.

The road in front of the house is located at a slightly higher elevation which could cause some ponding and increased runoff in the direction of the house. Figure 5.1 depicts the front view of the house which was retrofitted using geogrid.

The application of the geogrid reinforced plastering was selected based on the exceptional performance noticed during the flexural strength testing program. Figure 5.2 displays the procedure of retrofitting the walls in the demonstration house using geogrid.

The existing plaster of the external walls were detached to a height around 1 m as the initial step. After the plaster was removed, a groove was cut in the floor approximately 15 mm away from the wall and removing the concrete in-between to a depth of 50 mm.

The geogrid was then placed in the groove with due consideration to bend the bottom aperture along the longitudinal rib so that the vertically aligned ribs are well in placed before epoxying the geogrid. Some parts of the geogrid were held to the wall using a tape for a short period of time until the epoxy gets cures.

After that an initial 7 -10 mm scratch coat of plaster was applied to the wall before embedding the geo grid. The geogrid was then inserted into the rough coat before an additional topcoat is applied to the wall. Final thickness of the rendering was approximately 17.5mm which was similar to the thickness used in the experimental program. The reinforced rendering retrofit is applied to all exterior walls and covered 12 inches along any partitioning walls in order to reinforce the corners.



*Figure 5. 1:* Front view of the model house



(a) Removal of existing plaster



(b) Epoxy the geogrid in place



(c) Curing of epoxy



(d) Application of scratch coat and epoxied geogrid



(e) Final coat of rendering after embedding the geogrid

*Figure 5. 2: Procedure of retrofitting with geogrid*



## **6. CONCLUSION AND FUTURE WORK**

### **6.1 Conclusion**

It can be declared that according to the aforementioned results which were obtained from the experimental program conducted for the masonry wall panels made by FCB and CB that the flexural strength (parallel to bed joint) of the wall specimens have been increased considerably due to the retrofitting of the wall panels.

Results show that the flexural strength of saturated FCB wall panels retrofitted with geogrid has been increased up to 9.2 times and 5.81 times of the reference wall which is without retrofitting and rendering subjected to saturated condition for FCB and CB wall panels respectively.

The strength reduction due to saturation of wall panels which represents the saturation of walls due to flooding was also minimized by introducing the retrofitting to the masonry wall panels. Wall panels retrofitted with geogrid resulted 14.4% and 17% of strength reduction due to saturation for FCB and CB wall panels respectively and for wire mesh it was 33% and 30%.

This summarizes that the geogrid has been performed best as a retrofitting material than the wire mesh. However, wire mesh has also given an appreciable result. After the initial cracking of retrofitted walls, small scale cracks were appeared throughout the rendered face. It can be deduced that wall with retrofitting was able to increase the flexural capacity of the structural system by releasing the energy through crack propagation. Therefore, retrofitting of masonry walls by using geogrid and wire mesh can effectively increase the lateral load carrying capacity of masonry walls in both dry and saturated conditions. This will be directly linked to the community in flood prone areas of Sri Lanka and the outcome of this study will be helpful to minimize the risk of failure in URM structures (specifically walls) due to floods and ensure safe of the people during the flood situations hence it would increase the resistance to floods.

## **6.2 Future work**

In this study, feasibility of the retrofitting type was evaluated in terms of the flexural strength. Therefore, in addition to flexural strength, following characteristics can be also considered in further studies when selecting a suitable retrofitting type for URM structures.

1. Availability
2. Cost
3. Mesh Roughness
4. Thickness of the mesh (Without making plaster difficult to apply)
5. Flexibility (Buildability)

However, further research works have to be carried out in order to identify different kinds of materials that can be used to strengthen the existing walls by considering some of the aforementioned parameters such as availability and cost. Furthermore, research studies can be carried out in order to find the potential of utilizing the aforementioned retrofitting technique against other types of natural hazards like high winds (Storms) and expansive ground conditions.

## REFERENCES

1. Acreya, A., Czajkowski, J., Botzen, W., Bustamante, G., Campbell, K., Collier, B., Ianni, F., Kunreuther, H., Kerjan, E.M., & Montgomery, M. (2017). Adoption of flood preparedness actions: A household level study in rural communities in Tabasco, Mexico. *International Journal of Disaster Risk Reduction*, 24, 428–438.  
<https://doi.org/10.1016/j.ijdr.2017.05.025>
2. Alcocer, S. M., Ruiz, J., Pineda, J. A., & Zepeda, J. A. (1996). Retrofitting of confined masonry walls with welded wire mesh. *11<sup>th</sup> world conference on earthquake engineering, Mexico*, 1209.
3. Amiraslazadeh, R., Ikemoto, T., Miyajima, M., & Fallahi, A. (2012). A comparative study on seismic retrofitting methods for unreinforced masonry brick walls. *21<sup>st</sup> World Conference on Earthquake Engineering, Canada*, 3658.  
[https://www.iitk.ac.in/nicee/wcee/article/WCEE2012\\_3658.pdf](https://www.iitk.ac.in/nicee/wcee/article/WCEE2012_3658.pdf)
4. Bartolomé, Á. S., Quiun, D., & Zegarra, L. F. (2004). Effective system for seismic reinforcement of adobe houses. *13th World Conference on Earthquake Engineering, Canada*, 3321.  
[https://www.iitk.ac.in/nicee/wcee/article/13\\_3321.pdf](https://www.iitk.ac.in/nicee/wcee/article/13_3321.pdf)
5. Bernat, E., Gil, L., Roca, P., & Escrig, C. (2013). Experimental and analytical study of TRM strengthened brickwork walls under eccentric compressive loading. *Construction and Building Materials*, 44, 35–47.  
<https://doi.org/10.1016/j.conbuildmat.2013.03.006>
6. Bhattacharya, S., Nayak, S., & Dutta, S. C. (2014). A critical review of retrofitting methods for unreinforced masonry structures. *International Journal of Disaster Risk Reduction*, 7, 51–67.  
<https://doi.org/10.1016/j.ijdr.2013.12.004>
7. British Standards. (1999). “Methods of test for masonry. Determination of compressive strength”. BS EN 1052-1:1999.
8. British Standards. (1999). “Methods of test for mortar for masonry. Determination of consistence of fresh mortar (by flow table)”. BS EN 1015-3:1999.

9. British Standards. (1999). “Methods of test for mortar for masonry. Determination of flexural and compressive strength of hardened mortar”. BS EN 1015-11:1999.
10. Bhattacharjee, K., & Behera, B. (2018). Determinants of household vulnerability and adaptation to floods: Empirical evidence from the Indian State of West Bengal. *International Journal of Disaster Risk Reduction*, 31, 758–769.  
<https://doi.org/10.1016/j.ijdr.2018.07.017>
11. Bischof, P., & Suter, R. (2014). Retrofitting Masonry Walls with Carbon Mesh. *Polymers*, 6(2), 280–299.  
<https://doi.org/10.3390/polym6020280>
12. Blondet, M., Torrealva, D., Vargas, J., Velásquez, J., & Tarque, N. (2006). Low cost reinforcement of earthen houses in seismic areas. *The 14<sup>th</sup> World Conference on Earthquake Engineering, China*.  
[https://www.iitk.ac.in/nicee/wcee/article/14\\_09-02-0001.PDF](https://www.iitk.ac.in/nicee/wcee/article/14_09-02-0001.PDF)
13. British Standards. (2005). “Eurocode 6: Design of masonry structures — Part 1-1: *General rules for reinforced and unreinforced masonry structures*.” BS EN 1996-1-1:2005.
14. British Standards. (2012). “UK National Annex to Eurocode 6: Design of masonry structures – Part 1-1: *General rules for reinforced and unreinforced masonry structures*.” NA BS EN 1996-1-1:2012.
15. British Standards. (2015). “Methods of test for masonry units. *Determination of compressive strength*”. BS EN 772-1: 2015.
16. British Standards. (2016). “Methods of test for masonry. *Determination of flexural strength*”. BS EN 1052-2:2016.
17. Dewan, T. H. (2015). Societal impacts and vulnerability to floods in Bangladesh and Nepal. *Weather and Climate Extremes*, 7, 36–42.  
<https://doi.org/10.1016/j.wace.2014.11.001>
18. De Silva, M. M. G. T., & Kawasaki, A. (2018). Socioeconomic Vulnerability to Disaster Risk: A Case Study of Flood and Drought Impact in a Rural Sri-Lanka Community. *Ecological Economics*, 152, 131–140.

<https://doi.org/10.1016/j.ecolecon.2018.05.010>

19. Delgrange, E., & Adeyeye, K. (2018). Decision-Support Tool for Retrofittable Flood Resilience. *Procedia Engineering*, 212, 847–854.  
<https://doi.org/10.1016/j.proeng.2018.01.109>
20. Dias, P., Arambepola, N. M. S. I., Weerasinghe, K., Weerasinghe, K. D. N., Wagenaar, D., Bouwer, L. M., & Gehrels, H. (2018). Evaluating adaptation measures for reducing flood risk: A case study in the city of Colombo, Sri Lanka. *International Journal of Disaster Risk Reduction*, 37, 101162.  
<https://doi.org/10.1016/j.ijdr.2019.101162>
21. Dias, P., Arambepola, N. M. S. I., Weerasinghe, K., Weerasinghe, K. D. N., Wagenaar, D., Bouwer, L. M., & Gehrels, H. (2018). Development of damage functions for flood risk assessment in the city of Colombo (Sri Lanka). *Procedia Engineering*, 212, 332-339.  
<https://doi.org/10.1016/j.proeng.2018.01.043>
22. Dissanayake, P., Hettiarachchi, S., & Siriwardana, C. (2018). Increase in Disaster Risk due to inefficient Environmental Management, Land use policies and Relocation Policies. Case studies from Sri Lanka. *Procedia Engineering*, 212, 1326–1333.  
<https://doi.org/10.1016/j.proeng.2018.01.171>
23. Ehsani, M. R., Saadatmanesh, H., & Velazquez-Dimas, J. I. (1999). Behavior of retrofitted URM walls under simulated earthquake loading. *Journal of Composites for Construction*, 3(3), 134–142.  
[https://doi.org/10.1061/\(ASCE\)1090-0268\(1999\)3:3\(134\)](https://doi.org/10.1061/(ASCE)1090-0268(1999)3:3(134))
24. ElGawady, M A, Lestuzzi, P., & Badoux, M. (2006). Retrofitting of Masonry Walls Using Shotcrete. *Annual technical conference in New Zealand Society for Earthquake Engineering*, 45.  
<http://db.nzsee.org.nz/2006/Paper45.pdf>
25. ElGawady, Mohamed A., Lestuzzi, P., & Badoux, M. (2005). Aseismic retrofitting of unreinforced masonry walls using FRP. *Composites Part B: Engineering*, 37(2), 148–162.  
<https://doi.org/10.1016/j.compositesb.2005.06.10>

26. Farooq, S., Ilyas, M., & Amir, S. (2012). Response of Masonry Walls Strengthened with CFRP and Steel Strips. *Arabian journal for science and engineering*, 37(3).  
<https://10.1007/s13369-012-0190-9>
27. Ferreira, S. (2011). Nature, Socioeconomics and Flood Mortality. *Institute of Technology, Georgia water resources institute. Georgia*.  
<https://smartech.gatech.edu/handle/1853/46292>
28. Kelman, I., & Spence, R. (2003). A limit analysis of unreinforced masonry failing under flood water pressures. *Masonry International*, 16, 51–61.
29. Kundzewicz, Z., Su, B., Wang, Y., Xia, J., Huang, J., & Jiang, T. (2019). Flood risk and its reduction in China. *Advances in Water Resources*, 130, 37–45.  
<https://doi.org/10.1016/j.advwatres.2019.05.020>
30. Macabuag, J., Guragain, R., & Bhattacharya, S. (2012). Seismic retrofitting of non-engineered masonry in rural Nepal. *Proceedings of the Institution of Civil Engineers - Structures and Buildings*, 165(6), 273–286.  
<https://doi.org/10.1680/stbu.10.00015>
31. Mansourikia, M. T., & Hoback, A. (2014). Retrofit of unreinforced masonry walls using geotextile and CFRP. *Electronic Journal of Structural Engineering*, 14, 50–56.
32. Mendis, W. S. W., Silva, S. D., & Silva, G. H. M. J. D. (2014). Performance and Retrofitting of Unreinforced Masonry Buildings against Natural Disasters – A Review Study. *Engineer: Journal of the Institution of Engineers, Sri Lanka*, 47(3), 71–82.  
<https://doi.org/10.4038/engineer.v47i3.6896>
33. Jamali, B., Lowe, R., Bach, P. M., Urich, C., Arnbjerg-Nielsen, K., & Deletic, A. (2018). A rapid urban flood inundation and damage assessment model. *Journal of Hydrology*, 564, 1085–1098.  
<https://doi.org/10.1016/j.jhydrol.2018.07.064>

34. Luino, F., Turconi, L., Paliaga, G., Faccini, F., & Marincioni, F. (2018). Torrential floods in the upper Soana Valley (NW Italian Alps): Geomorphological processes and risk-reduction strategies. *International journal of Disaster Risk Reduction*, 27, 343–354.  
<https://doi.org/10.1016/j.ijdr.2017.10.021>
35. Mahmood, S., Khan, A. ul H., & Ullah, S. (2016). Assessment of 2010 flash flood causes and associated damages in Dir Valley, Khyber Pakhtunkhwa Pakistan. *International Journal of Disaster Risk Reduction*, 16, 215–223.  
<https://doi.org/10.1016/j.ijdr.2016.02.009>
36. Pathak, S., & Ahmad, M. M. (2018). Role of government in flood disaster recovery for SMEs in Pathumthani province, Thailand. *Natural Hazards*, 93(2), 957–966.  
<https://doi.org/10.1007/s11069-018-3335-7>
37. Qasim, S., Qasim, M., Shrestha, R., Khan, A., & Tun, K. (2016). Community resilience to flood hazards in Khyber Pukhthunkhwa province of Pakistan. *International Journal of Disaster Risk Reduction*, 18.
38. Samarakoon, U., & Abeykoon, W. (2018). Emergence of Social Cohesion after a disaster. *Procedia Engineering*, 212, 887–893.  
<https://doi.org/10.1016/j.proeng.2018.01.114>
39. Sung, E., Li, H. M. D., & Nam, J. (2015). Overview of natural disasters and their impacts on Asia and the Pacific 1970-2014. *United Nations Economic and Social commission for Asia and the Pacific, Thailand*.  
<https://www.unescap.org/resources/overview-natural-disasters-and-their-impacts-asia-and-pacific-1970-2014>
40. Ullah, R., Shivakoti, G., & Ali, G. (2015). Factors Effecting farmers' risk attitude and risk Perceptions: The case of Khyber Pakhtunkhwa Pakistan. *International Journal of Disaster Risk Reduction*, 13.
41. Win, S., Zin, W. W., Kawasaki, A., & San, Z. M. L. T. (2018). Establishment of flood damage function models: A case study in the Bago River Basin, Myanmar. *International Journal of Disaster Risk Reduction*, 28, 688–700.  
<https://doi.org/10.1016/j.ijdr.2018.01.030>